

Modeling the contribution of lamina 5 neuronal and network dynamics to low frequency EEG phenomena

Fadi N. Karamneh · Munther A. Dahleh ·
Emery N. Brown · Steve G. Massaquoi

Received: 15 February 2005 / Accepted: 24 May 2006 / Published online: 8 August 2006
© Springer-Verlag 2006

Abstract The Electroencephalogram (EEG) is an important clinical and research tool in neurophysiology. With the advent of recording techniques, new evidence is emerging on the neuronal populations and wiring in the neocortex. A main challenge is to relate the EEG

Electronic Supplementary material Supplementary material is available in the online version of this article at <http://dx.doi.org/10.1007/s00422-006-0090-8>

Sensorimotor Control Project- MIT Harvard NeuroEngineering Research Collaborative.

F. N. Karamneh (✉)
Department of Electrical and Computer Engineering,
American University of Beirut, Beirut 1107-2020, Lebanon
e-mail: fk14@aub.edu.lb

M. A. Dahleh · S. G. Massaquoi
Department of Electrical Engineering and Computer
Science, Massachusetts Institute of Technology,
Cambridge, MA 02139, USA

E. N. Brown
Department of Brain and Cognitive Sciences,
MIT-Harvard Division of Health Science and Technology,
Massachusetts Institute of Technology,
Rm 46-6079, 77 Massachusetts Ave,
Cambridge, MA 02139, USA

E. N. Brown
Neuroscience Statistics Research Laboratory,
Department of Anesthesia and Critical Care,
Massachusetts General Hospital,
55 Fruit Street Clinics 3,
Boston, MA 02114, USA

S. G. Massaquoi
Massachusetts Institute of Technology,
MIT-Harvard Division of Health Sciences and Technology,
Rm 32-214, 77 Massachusetts Ave,
Cambridge, MA 02139, USA

generation mechanisms to the underlying circuitry of the neocortex. In this paper, we look at the principal intrinsic properties of neocortical cells in layer 5 and their network behavior in simplified simulation models to explain the emergence of several important EEG phenomena such as the alpha rhythms, slow-wave sleep oscillations, and a form of cortical seizure. The models also predict the ability of layer 5 cells to produce a resonance-like neuronal recruitment known as the augmenting response. While previous models point to deeper brain structures, such as the thalamus, as the origin of many EEG rhythms (spindles), the current model suggests that the cortical circuitry itself has intrinsic oscillatory dynamics which could account for a wide variety of EEG phenomena.

1 Introduction

The scalp electroencephalogram (EEG) is a spatially filtered version of the underlying cortical field potentials. Despite the advent of other recording techniques, EEG remains an attractive modality due to its non-invasiveness (scalp electrodes) and ability to convey real-time information about the brain state of wakefulness for extended periods of time. As such, EEG is used clinically to study sleep disorders (Sinton and McCarley 2000), to analyze brain behavior under seizures (Mormann et al. 2006), and to follow the level of consciousness under anesthesia (Tung 2005). It is furthermore used in research to define the neurophysiological correlates of established behavior such as cognitive processing (Mima et al. 2001; Tallon-Baudry and Bertrand 1999), auditory response, eye movement, and memory formation (Klimesch 1999).

Despite its extensive use, the mechanisms underlying EEG generation are less well understood and remain an active research question in neuroscience. As EEG represents aggregate electric field potential that emanates primarily from the outer layer of the cortex (neocortex) (Nunez 1981; Destexhe et al. 1999), the challenge is to explain EEG phenomena characteristic of specific brain states in terms of the associated firing activity in neocortical circuits. Ideally, the circuit behavior can be also understood in terms of the information processing that is likely to be taking place.

Earlier work in this area varied from very basic, such as representing EEG as emanating from abstract current sources (Nunez 1995; Wright and Liley 1995), to rhythm-specific (thalamic spindle activity in Contreras et al. 1997; alpha rhythms in Jones et al. 2000; sleep in Compte et al. 2003; Timofeev et al. 2000) in the sense that the models were not clearly compatible with models explaining different rhythms.

A salient feature of the majority of such modeling efforts is that the rhythmicity of EEG was due primarily to the action of deeper brain structures such as the thalamus or hippocampus (Bazhenov et al. 1998a,b; Contreras et al. 1997; Destexhe et al. 1996). The neocortex is presumed to simply reflect oscillations passively without major intrinsic oscillatory dynamics.

While a number of EEG rhythms and signals (e.g. sleep spindles) have been demonstrated to have a thalamic origin, it has been suspected that other rhythms have at least a significant cortical contribution since these were sustained in athalamic animals. However, the nature of this contribution has not been characterized heretofore.

In the current work, we look at phenomenological, anatomic, and neurophysiological evidence from the cortical circuit itself to understand its intrinsic oscillatory properties. We devise simplified wiring and neuronal diagrams of the neocortex at three spatial scales that emphasize the intrinsic dynamics of large cells in layer 5, known as tufted layer 5 cells (TL5 in short). We illustrate how this architecture and the associated dynamical behavior can be used to study well known EEG rhythmicities such as the alpha rhythms (~ 10 Hz) observed over the visual areas under attentional idling conditions (reviewed in Lopes Da Silva 1991), the slow-wave sleep (< 1 Hz) which is recorded in later stages of deep sleep (reviewed in Steriade et al. 2001), and a type of cortical seizure that results from disinhibition of cortical neurons (Castro-Alamancos 2000). The simulated model of layer 5 neurons replicates experimental data under the aforementioned brain states. It furthermore predicts a form of increased excitability under repetitive ~ 10 Hz stimulation of cortical

tissue, known as the augmenting response, and thought to be an effective “start-up” or recruitment mechanism by which large neuronal populations may be quickly recruited by cortical or subcortical inputs (Castro-Alamancos and Connors 1996a,b; Bazhenov et al. 1998; Gernier et al. 1998).

Accordingly, the presented modeling framework represents a coherent test-bed for a wide range of slow EEG oscillatory rhythms (< 15 Hz), and that is in agreement with a large repertoire of recent psychological, anatomical, and neurophysiological evidence (cellular and system levels).

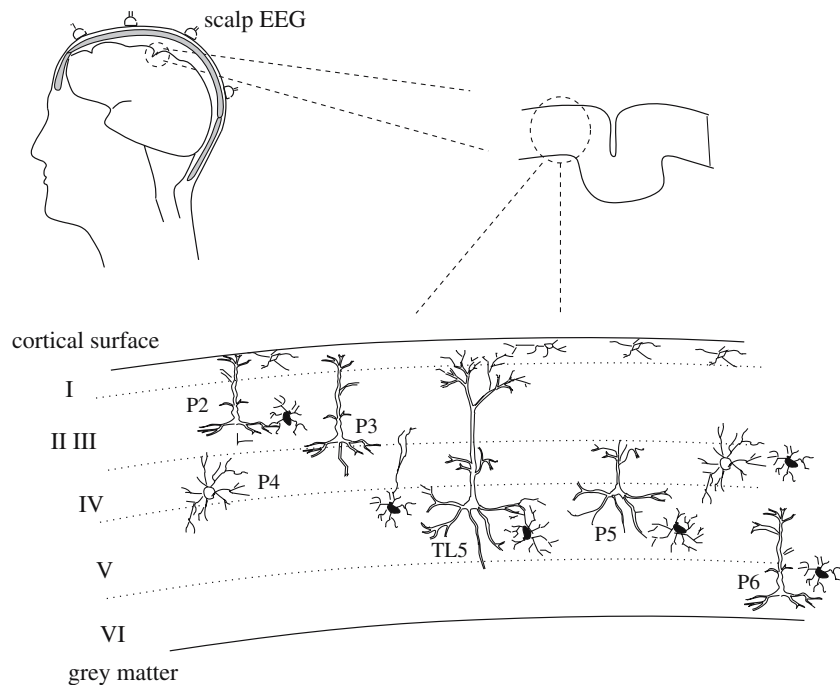
In the next section, we outline the proposed basic cortical circuit along with supporting evidence at the cellular and network level. We then develop mathematical models of various cells based on a simplified Hodgkin–Huxley formulation of neuronal models, and then summarize the principal dynamics of this cortical circuit. These models are used next to explain the emergence of augmenting responses, alpha waves, slow-wave sleep and disinhibition-induced seizures. We conclude by highlighting the implications and limitations of this framework for cortical rhythm modeling.

2 Materials and methods

2.1 Cortical model

The neural populations of the cerebral cortex vary in complexity and functionality among various cognitive systems. We will therefore seek to reduce such complexity by adopting the simplest structure widely believed to exist as an underlying skeleton in the neocortex. In particular, we adopt the segregation of neocortical neural populations according to mainly six cortical lamina or layers (Mountcastle 1998) that lie parallel to the cortical surface (Fig. 1). Such layers are distinguished by the anatomical and electrophysiological properties of their constituent neurons. The superficial layers of the neocortical model (layers 1–3) will be constructed from basic regularly spiking excitatory pyramidal cells (nearly uniformly-timed firing). The middle layer 4, existing mainly in sensory systems, will consist of excitatory spiny stellate cells. The deep layers (layers 5, 6) have the regularly spiking pyramidal cells in addition to a specialized form of pyramidal cell known as the tufted layer 5 cell (TL5) which can act as regularly spiking or bursting cell, to be detailed later. Finally, the model will include the inhibitory interneurons that exist in all layers and act to control excitation of various pyramidal cell populations.

Fig. 1 Schematic of the different scales involved in EEG generation. *Top* Scalp EEG recording and neocortical depth slice. *Bottom* Laminar distribution of representative cellular populations in the neocortex. Note that thickness is not to scale



2.1.1 Salient horizontal connectivity

The model describes emergent rhythms based on interaction between cortical neuronal networks organized at three spatial scales of horizontal connectivity. (Figs. 2–4).

- (a) At the finest scale is the *cortical column*, which is a well documented aggregation of neurons extending to about 0.1–0.3 mm in diameter and defined by the spatial spread of specific driving inputs arriving at the middle cortical layer 4 (in sensory cortices, these inputs arrive from modality-specific thalamic nuclei such as the LGN in the visual system or from distant cortical areas). In the current model, neuronal populations of various layers within a cortical column are represented simply by a single neuron of each basic type (Figs. 2–4) since evidence suggest strong synchronization to exist within a cortical column [apparently mediated by mechanisms such as interneuronal electrical coupling (Tamas et al. 2000), and facilitated neuronal connectivity (Feldmeyer and Sakmann 2000)].
- (b) At the intermediate scale is a circuit that we introduce here and term the *local columnar assembly LCA* shown in Fig. 2. This is defined by the spatial extent of horizontal excitatory connections between layer 5 neurons of the neocortex (Feldmeyer and Sakmann 2000; Markram 1997), and as such can include groups of connected cortical columns (previous scale) up to a diameter of 1–2 mm (see also below).

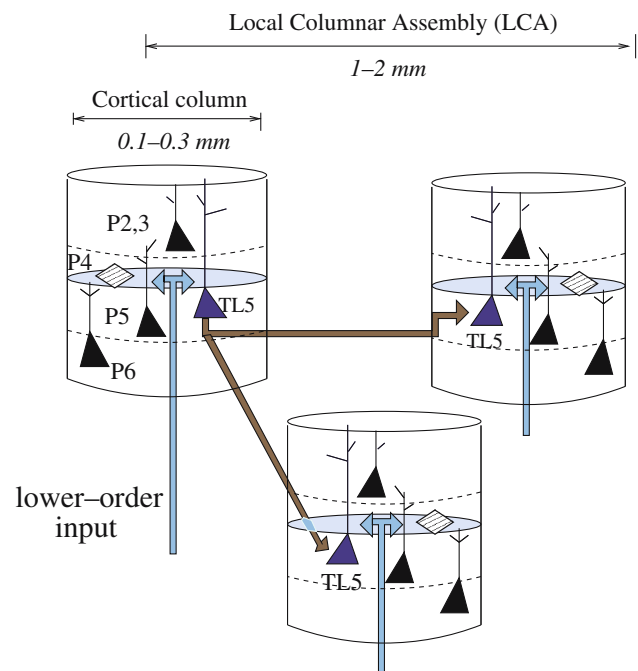


Fig. 2 Two spatial scales of the model. The cortical column is defined by horizontal spread of middle layer 4 input (0.1–0.3 mm in diameter). The local columnar assembly (*LCA*) is defined by the horizontal spread of TL5 neuron connections (1–2 mm in diameter)

- (c) At the coarsest scale is what we term the *inter-areal columnar assembly ICA* shown in Fig. 3. This describes connectivity between cortical columns, and thereby implicitly between portions of column assemblies, belonging to distant cortical areas (> 2 mm). While the previous scales were mediated

Fig. 3 Final spatial scale of the model. The inter-areal columnar assembly (ICA) is defined by the long-range (cortico–cortical) connections arriving in middle layers (feedforward) or the upper layers (feedback) and is of > 2 mm in length

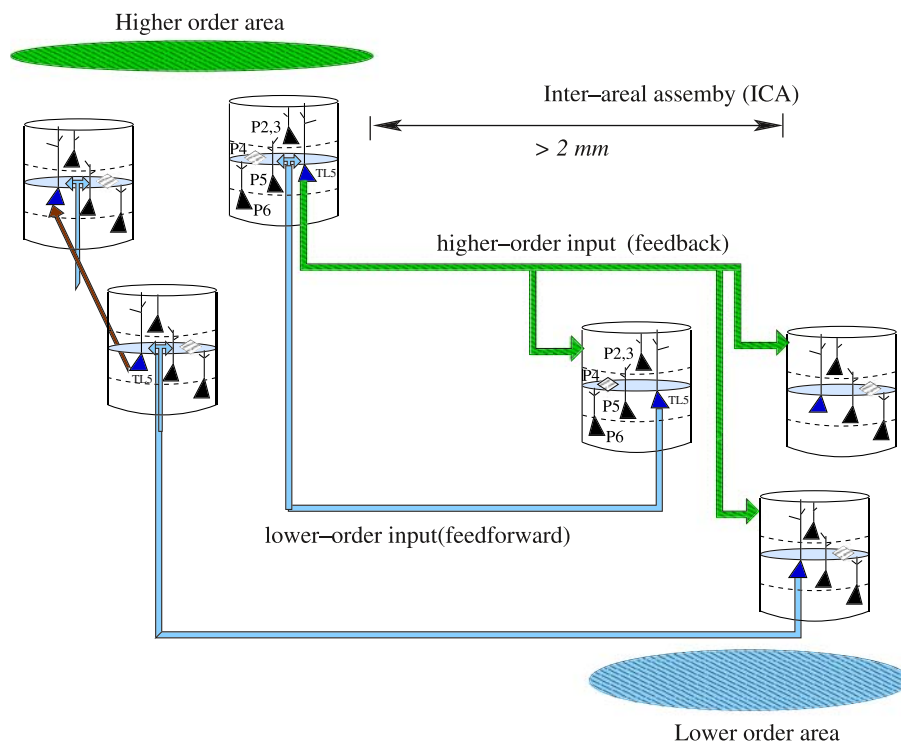
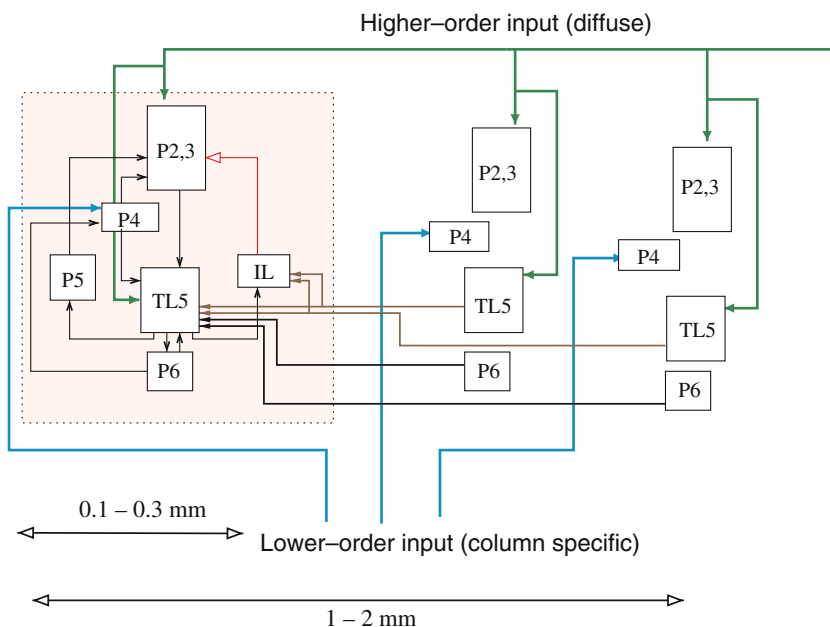


Fig. 4 Major connectivity inside a cortical column (left) and at the local columnar assembly (LCA) scale. All connections shown are excitatory, except for IL (intralaminar interneuron) to P2,3 connection which is inhibitory. Within a column, TL5 cells receive input from other layers as shown and provide inhibitory feedback to layers 2,3. At the LCA scale, TL5 neurons receive connections from TL5 neurons and layer 6 neurons of other columns. Long-range inputs are either to the middle or upper layers (as in Figs. 2,3)



by axonal branching inside the neocortex, connectivity at this scale is mediated by long axons going into the grey matter and are known as cortico–cortical fibers.

In general, cortico–cortical connections have been best characterized in sensory systems and are usually initiated and terminated in specific cortical layers. This restricted connectivity is especially clear when two

cortical areas form a hierarchy of information transfer (Mountcastle 1998; Fellman and Van Essen 1991); that is, when one “lower-order” area lies closer to the input sensory origin (e.g. early visual processing stage) while the other “higher-order” area lies further downstream (later visual processing). In this case, evidence shows two distinct patterns of cortico–cortical connections: (1) lower-to-higher order or *ascending (feedforward)* inputs arriving mainly at the middle cortical layers (layer

4 and lower layer 3) and are spatially restricted to the cortical column (the lowest scale of the model), and (2) higher-to-lower order or *descending (feedback)* inputs avoiding middle layers, arriving at the superficial layers 1–2 (and possibly deep layer 5) and are more spatially diffused (Fellman and Van Essen 1991; Callaway 1998; Cauller et al. 1998) beyond the boundaries of a single column (the local columnar assembly scale of the model).

2.1.2 Salient vertical connectivity

We will next describe the major pathways which connect cells of different laminar origin at the three horizontal scales introduced above.

- (a) The circuit associated with the lowest horizontal scale (functional column, Fig. 4) emphasizes the following interlaminar or vertical connections. First, a strong pathway exists from pyramidal cells in layer 3 (P2,3) to large Tufted Layer 5 cells (TL5), but not smaller cells of deeper layer 5 (P5), and is focused within a functional column spatial extent (Thomson and Deuchars 1997; Schubert et al. 2001; Kaneko et al. 2000). Excitatory feedback into layer 3, on the other hand, originates from smaller layer 5 (regularly spiking) cells P5 (Callaway 1998). We also utilize various experimental evidence (Mountcastle 1998) to support the existence of layer 5 to layer 6, layer 6 to layers 5 and 4, and layer 4 to layer 5 connections. Also at this scale, an inhibitory pathway from layer 5 to layer 3 is incorporated (discussed below) and mediated by interneurons located in layer 5 (IL in Fig. 4).
- (b) The vertical connectivity associated with the intermediate (local columnar assembly) scale consisted mainly of layer 6 pyramidal cells (P6, Fig. 4) targeting TL5 but not smaller RS cells P5 in layer five (Schubert et al. 2001).
- (c) Finally, vertical connections at the largest scale follow layer-specific topology, as mentioned earlier. In particular, if two interacting areas are of the same order, connectivity is restricted to be within the same layer (e.g. layer 3 to layer 3). Interactions between different order areas, however, can be either ascending or descending. We consider ascending connections to originate from layers 3 and 5 and to target the middle layer 4 (P4) of the higher order area. Descending connections, on the other hand, originate from layer 5 pyramidal cells

and target layers 1 and 5 (P2,3 and TL5) of the lower order area, as shown in Fig. 4.

2.1.3 Layer 5 properties

At least two distinct types of pyramidal cells exist in layer five of the neocortex (Feldmeyer and Sakmann 2000; Markram 1997; Williams and Stuart 1999). The first, or tufted layer 5 cells (TL5), are large with thick apical dendritic tuft reaching into superficial cortical layers 1 and 2 (TL5 in Fig. 1). The second are smaller with thin dendritic tuft reaching middle cortical layers (P5). The distinction is based on morphology, synaptic targets and firing characteristics. The model we present places special emphasis on TL5 cells, as follows.

- (a) **Intra-columnar connectivity:** Within their immediate neighborhood in a cortical column, TL5 cells are reciprocally connected to key pyramidal cell populations across cortical depth and thus have access and are able to modify the output of both superficial (layers 2,3) and deep infragranular (layers 5,6) pyramidal cell populations (Schubert et al. 2001).
- (b) **Intra-layer connectivity:** Within their own layer, TL5 cells form an extensively-connected network of neurons which goes beyond the functional boundaries of a single cortical column (Feldmeyer and Sakmann 2000; Markram 1997; Thomson and Bannister 1998) up to distances of 1–2 mm. These connections are especially strengthened, enhanced or facilitated between TL5 cell pairs undergoing bursting (Williams and Stuart 1999; Galarreta and Hursting 2000). In fact, it is these enhanced activation patterns under bursting that lead us to define the local columnar assembly LCA scale.
- (c) **Inter-laminar inhibition:** An inhibitory pathway from layer 5 to layer 3 pyramidal cells exists (IL in Fig. 4) and is selectively activated during active cognitive states thus controlling the output of superficial layers 2, 3 (Xiang et al. 1998; Kawaguchi and Kubota 1997). This pathway is likely mediated by a specialized interneuron type known as low threshold spiking interneurons (LTS) whose activation requires high frequency synaptic inputs (Thomson and Deuchars 1997; Goldberg et al. 2004). Inhibition within layer 5, on the other hand, could be mediated by a network of fast spiking (FS) interneurons which modulate the firing properties of both layer 5 pyramidal cells and LTS neurons. Note that electrical coupling within this FS interneuronal network could also promote

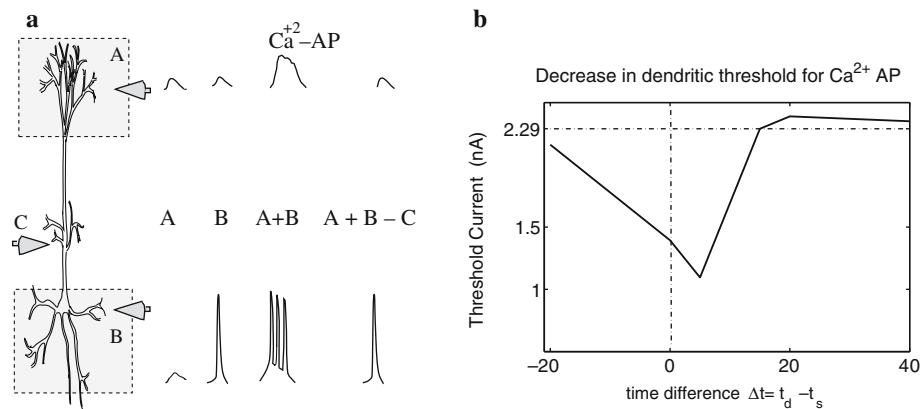


Fig. 5 Firing dynamics of TL5 cells. **(a)** inputs applied to three dendritic zones amplify or suppress the ability of a TL5 cell to burst. Inputs to zone A provide little injected current into the soma, inputs to zone B could result in regular firing in that cell. A coupling of both inputs within 20 ms, however, causes a dendritic Calcium action potential Ca^{2+} with a corresponding burst at the

cell axonal output. Zone C acts as a bottleneck between the two zones. **(b)** Simulated window of facilitation over which the threshold for bursting is reduced. Plotted here is the reduction in the threshold dendritic depolarization V_{th} as a function of the time difference $\Delta t = t_d - t_s$. (see text, curve based on experimental results of Larkum et al. 1999a)

synchronization between pyramidal cells within a cortical column (Tamas et al. 2000) but is not modeled here.

- (d) **Firing dynamics—Bursting:** While small pyramidal cells in layer 5 are of the regularly spiking type (P5), the larger cells TL5 can fire in either a regularly spiking mode or a bursting mode (2–4 spikes per burst). The change in TL5 cell firing depends on neuromodulating currents (Wang and McCormick 1993) as well as on the synaptic input patterns into three main dendritic zones of these cells (Williams and Stuart 1999; Larkum et al. 1999a,b; Schwindt and Crill 1999) as shown in Fig. 5a: the apical dendritic tuft (zone A), the basal dendritic tuft (zone B) and the middle dendritic area (zone C). While synaptic inputs to distal zone A provide little injected current into the soma (and are thus electrically distant), inputs to zone B could result in regular firing in the cell due to proximity of this zone to the soma. In this case, the cell regular firing y_{reg} can be approximated by the relationship

$$y_{\text{reg}} = \begin{cases} 1, & \text{if } R_b I_B > V_R \\ 0, & \text{else,} \end{cases} \quad (1)$$

where I_B is the current applied to zone B, R_b is the associated gain, and V_R is the regularly spiking threshold.

Interestingly, when inputs are applied to both zones A and B within a ~ 20 ms time window, a burst of action potentials is produced in the cell. Moreover, this

bursting occurs at a lower threshold than that required if either input to zone A or B is applied alone. Here, zone C acts as a bottleneck between the two zones A and B in that it either facilitates or inhibits the cells ability to burst. Such a mechanism can be thought of as a logical gating relationship. Assuming that an input to zone A injects current I_A at time t_d and another input to zone B injects current I_B at time t_s , then the cell bursting behavior y_{burst} can be approximated as

$$y_{\text{burst}} = \begin{cases} 1, & \text{if } (1 + K_c I_C)(K_a I_A + K_b I_B) > V_{\text{th}}(t_d - t_s) \\ 0, & \text{else,} \end{cases} \quad (2)$$

where I_m is the input to zone m and K_m is the associated gain ($m = \{A, B, C\}$). In Eq. (2), y_{burst} depends on a threshold voltage V_{th} which varies depending on t_d and t_s the time of arrival of inputs to zones A and B, respectively. Inputs I_C to zone C modulate the cell ability to reach bursting threshold according to K_c . Physically, a burst is essentially produced when a Calcium action potential (Ca^{2+} -AP) is generated in the dendritic zone A and propagates to the soma. This dendritic Ca^{2+} -AP is aided by a back propagating somatic action potential (BAC) and enhanced/reduced by middle zone C inputs. The function $V_{\text{th}}(t_d - t_s)$ produces a time window of facilitation over which the threshold for bursting is reduced. Figure 5b shows such reduction in the threshold dendritic depolarization required to induce dendritic Ca^{2+} -AP and subsequently somatic burst generation (Larkum et al. 1999). Recent experimental recordings under in vivo-like conditions have shown that such coupling between zones A and B in TL5 cells

indeed increase drastically the ability of apical arriving inputs in changing the firing patterns of TL5 cells (Larkum et al. 2004).

- (e) **Firing dynamics—Input amplification:** TL5 pyramidal neuron possesses a high gain amplification property under minimal input excitatory states, such as during sleep (Sanchez-Vives and McCormick 2000). This amplification occurs due to both (1) *reduced inhibition* under such states, and (2) a *rebound depolarization* property of TL5 cells. First, the level of inhibition have been reported to be lowered in at least one subpopulation of TL5 cells under reduced excitation states (Schubert et al. 2001; Hefti and Smith 2000) allowing such cells to be more active compared to neighboring cells. Second, TL5 cells have been shown to depolarize upon release from inhibition and to even produce action potentials (similar to depressing and then releasing a spring), a phenomenon known as *rebound depolarization* (shown in Fig. 7a). This behavior is mediated by the interplay between an intrinsic ionic current known as low threshold Ca^{2+} current I_T (Thomson and Deuchars 1997; Chen et al. 1996) with another inward current called hyperpolarization-activated cation current I_h (Burger et al. 2003).
- (f) **Circuit dynamics:** The essential features of layer 5 cells used here are, first, their greater excitability compared to cells in layers 2,3 (Schubert et al. 2001); second, their propensity, especially TL5 cells, to sustain oscillations around 10 Hz; and, third, their ability to spread synchronous activation within layer 5 between cortical columns to reach the columnar assembly scale (LCA) defined here. This is supported by several experiments. In slice preparations, TL5 cells were seen to have lower inhibition than regularly spiking cells in layers 2,3 (cat motor cortex in Van Brederode and Spain 1995) and in layer five (Schubert et al. 2001). Consequently, TL5 cells sustained emergent oscillations in the 8–10 Hz range under increased excitability (Spain et al. 1991) or unaltered excitability (optical recordings in Wu et al. 1999). Similar properties were recorded in behaving animals; in particular, in vivo experimental procedures in rats implicate a qualitatively similar role for layer 5 cells in signal propagation between cortical columns after whisker stimulation (Armstrong-James et al. 1992). Activation of layer 5 appeared to be spatially distributed (Ghazanfar and Nicolelis 1999), thus extending to the LCA

scale, and preceded that of the superficial layers (Brumberg et al. 1999).

2.1.4 Cellular models

For all simulations, reported here as either firing patterns or surface EEG, single model neurons were used to represent the collection of each principal type of neuron within a cortical column. Regular spiking neurons and interneurons (all of the FS variety) were modeled using a simplified version of the Hodgkin–Huxley formulation which we refer to as *Wilson-type models* (developed by Wilson 1999) with a single synaptic input zone per unit (see Supplementary Materials section for cellular and synaptic model details). TL5 cells, on the other hand, had two input zones, distal and basal, whose interaction dynamics replicated the switch in firing mode reported in the literature (Larkum et al. 1999a; Schwindt and Crill 1999). These cells also had somatic currents that produced rebound depolarization (Castro-Alamancos and Connors 1996a). In addition to the aforementioned Wilson-type models, we developed two-compartment Hodgkin–Huxley (H–H) models of TL5 cells with detailed channel dynamics of about 18 ionic currents. The H–H model of a TL5 cell, whose firing dynamics approximate experimental data (Larkum et al. 1999a; Schwindt and Crill 1999), was utilized in the single pair simulation of augmenting responses and served to emphasize the generality of our results when more detailed cell models are incorporated.

2.1.5 Framework of models versus single comprehensive model

Different EEG phenomena are produced by different neuronal and network dynamics at various levels of physical scale. To capture realistically all EEG behavior within a single model would require the simultaneous simulation of at least hundreds of physiologically realistic neurons. While being an eventual goal, a large-scale model easily obfuscates rather than clarifies the interactions essential for each phenomenon. Moreover, it may be too cumbersome to be used easily for study of specific conditions. On the other hand, a collection of mutually consistent simpler models that each emphasizes certain dynamics can afford great insight and computational tractability. We have therefore developed three separate but mutually consistent models for different EEG features. The first two models (AR-D) and (AR-A) simulated the augmenting response at two levels of neuronal details. The first (AR-D) utilized incorporated detailed Hodgkin–Huxley dynamics for cellular ionic

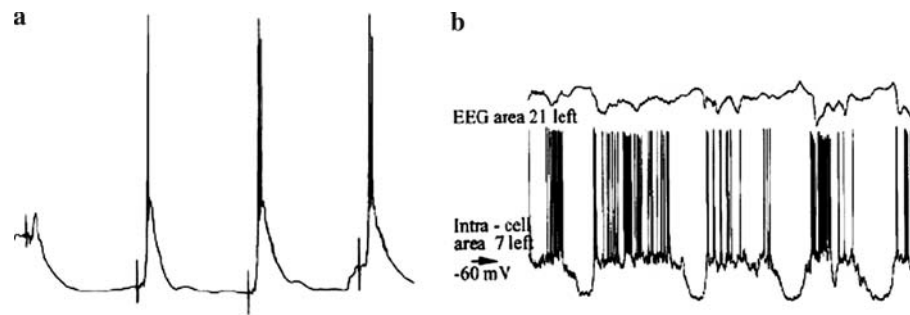


Fig. 6 **a** Experimental recording showing augmented responses (AR) in rat cortex. With each stimulus delivered (vertical line, 100 ms separation), cellular firing in layer 5 increases from 1 to 3 spikes per stimulus. Figure adapted from Castro-Alamancos and Connors (1996b) (Copyright 1996 by the Society for Neurosci-

ence). **b** Experimental recording of slow wave sleep EEG (top trace) and corresponding cellular recordings. Note the up and down states. Figure adapted from Steriade 2001 (with permission, Copyright 2001 by the American Physiological Society)

currents. The second (AR-A) used approximations of H–H dynamics to simulate the same phenomenon. The third and final model used the approximated H–H dynamics (thus termed A-HH) to simulate alpha, slow-wave sleep, and disinhibition induced seizures.

The simulations incorporate a minimal set of elements and several approximations needed to highlight major players in each rhythm. In several instances, we provide two different versions of a model (simplified or more detailed neurocircuit) to show the basic mechanisms that we believe are independent of omitted level of detail. The parameters of various models used to investigate each rhythm are given in the Supplementary Materials section.

2.2 Test rhythms

We will next briefly present a set of EEG rhythms which have been shown experimentally to be of mainly cortical origin. Therefore, our modeling framework will be able to reproduce such rhythms, at least qualitatively, and it will be consistent with recordings at both the cellular level and the EEG level.

2.2.1 Augmenting responses

Augmenting response (AR) refers to the increased depolarization and cortical activation observed under repetitive stimulation of a cortical set of neurons (Castro-Alamancos and Connors 1996a,b). ARs have been reported to occur in several cortical areas by delivering stimulus trains locally or to specific thalamic nuclei in the 10 Hz range as well as by stimulating the white matter or callosally-projecting fibers (across hemispheres) in athalamic animals (thalamus removed). Since ARs increase cortical activation, they are thought to have an important potential role in promoting short-

term plasticity in thalamocortical systems as well as in enhancing sustained activity in cortical networks (Nunez et al. 1993; Bazhenov et al. 1998a,b).

At the cellular level of rhythm generation, augmentation is manifested by bursting-like behavior in layer 5 cells and is maximally evoked in periods of sustained hyperpolarization. That is, such cells will burst, linked to AR, after having been inhibited for relatively long periods of time (Fig. 6a). At the network level, augmentation shows maximal spatial spread in layer 5 upon 10 Hz repetitive stimulation (Castro-Alamancos and Connors 1996b). The latter points to an integral role for bursting (TL5) cells in initiating, and possibly sustaining AR within the TL5 network of connected neurons.

2.2.2 Alpha-like rhythms

Alpha band activity is commonly recorded over the visual cortex under periods of unfocused attention and is especially prominent in eyes-closed, rest conditions (Lopes da Silva 1991). Visual alpha rhythms are thus referred to as *idling alpha* and have a dominant frequency of 8–10 Hz. Idling alpha disappears when eyes are open and the level of attention, or cortical activation is increased. Similar idling rhythms have been reported to occur over somatosensory cortex (mu rhythms) and auditory cortex (tau rhythms) (reviewed in Basar et al. 2001). Earlier experiments on visual alpha origins suggest that it could be represented by an equivalent dipole in upper layer 5 in the cortex of dogs, and is also possibly of cortical origin (Lopes da Silva 1991).

While the traditional view of alpha-band activity (8–12 Hz) has been that of an idling signature, more recent experiments point to a *different* form of alpha band rhythms located in the higher frequency band (10–12 Hz), and could possibly be related to early

recognition. As such, this new form of alpha is referred to as *functional alpha* rhythms (Basar et al. 2001).

2.2.3 Slow-wave sleep oscillations

Slow wave sleep rhythms occur during later stages of sleep (stages 3,4). These are characterized by a signature slow oscillatory cycle (<1 Hz) during which two states (up and down) of cellular activation alternate (reviewed in Steriade et al. 2001). During the first part of a cycle, the down state, there is a prominent EEG wave, that reflects a period of dominant neuronal silence or hyperpolarization (Fig. 6b). During the second part of a cycle, the up state, cells are highly active and tend to fire at increased frequencies which are in turn reflected at the EEG level as a progression of oscillations (spindles 10–14 Hz, followed by a beta range >20 Hz activity). Finally, the up state ceases and gives way to a period of neuronal silence, ending the slow-wave cycle.

Slow wave oscillations are of cortical origin since these have been reported to occur in athalamic animals in vivo (Steriade et al. 2001), as well as in situ cortical slices (Sanchez-Vives and McCormick 2000).

2.2.4 Disinhibition-induced seizures

Starting from a period of slow-wave sleep, EEG rhythms have been shown to progress to a form of characteristic spike-and-wave seizure when inhibition in the cortex is pharmacologically reduced. As shown in Fig. 15b, in the early stages of seizure formation, and by increasingly applying inhibitory receptor blockers, fast GABA_A inhibition in rat cortical tissue can induce spike-and-wave type seizures at low frequencies (traces 2–3 in Fig. 15b, Castro-Alamancos 2000). These are characterized by periods of neuronal silence (the down state inherited from the slow-wave sleep) followed by periods of fast runs (10–15 Hz) of the so-called paroxysmal depolarizing shifts (PDS, also shown in Steriade et al. 1998). If slow GABA_B inhibition is subsequently blocked (Fig. 15b, trace 4), the 10–15 Hz oscillations of PDS is sustained for longer runs. This type of spike-and-wave seizures is also cortical in origin since it was initiated in athalamic animals (Castro-Alamancos 2000).

3 Simulations and results

3.1 TL5 cell firing dynamics

The basic dynamical features of a tufted layer 5 TL5 cell were replicated for subsequent use in the circuit simulations. In particular, the developed cell model is

able to respond after release from inhibition with a rebound depolarization as observed in experiments (Castro-Alamancos 1996; Thomson and Deuchars 1996). This is shown in Fig. 7a (experimental) and c (model). In the simulated cell, various hyperpolarizing currents were applied in separate trials (at different times) and each lasted for 350 ms. After the injected current is removed, the cell can fire a single spike ($I_s = -0.4$ nA). Therefore, the high gain amplification of such cells is reproduced. In addition, we noted that bursting in this cell occurred after release from hyperpolarization when a depolarizing current I_d was applied to the dendritic compartment.

More importantly, the model TL5 cell can fire either single action potentials or bursts (3–4 spikes) depending on the coupling between zones A and B (as described earlier). The model replicates the decrease in threshold required for burst generation $V_{th}(t_d - t_s)$ observed in experiments (Larkum et al. 1999) and shown in Fig. 5b.

The model also qualitatively replicates further dynamic firing behavior of TL5 cells reported in (Schwindt and Crill 1999). In particular (Fig. 7b,d), by injecting increasingly high levels of depolarizing currents into the apical dendritic zone A of a TL5 cell, a sequence of bursts at 8–12 Hz is produced which then switched to regular spiking. Furthermore, this burst-to-regular firing switch occurred at increasingly earlier times as the level of the injected current to zone A is increased.

3.2 Augmenting responses

Augmenting responses were shown to be highly dependent on the stimulus delivery patterns onto the TL5 network. In particular, simulations show that the AR is maximally achieved, for the *same input stimulus strength*, when both apical and basal zones of TL5 cells (zones A and B in Fig. 5a) are activated concurrently either by thalamic or trans-callosal stimulation as detailed below.

3.2.1 Basic circuit AR demonstration

AR initiation was first studied at the most basic cellular level using a single pair of TL5 model neuron and an associated inhibitory interneuron IN (Fig. 8a). This simulation was done using the detailed Hodgkin–Huxley model of TL5 cells (AR-D) presented in the Supplementary Materials Section. The pair was subject to electrical stimulation at 10 Hz which in effect introduced excitation at either the basal or the apical dendritic zones of TL5 cell or both. A basal-arriving stimulus excited both TL5 cells (zone B) and IN interneuron while the apical-arriving stimulus was delivered only to TL5 cell

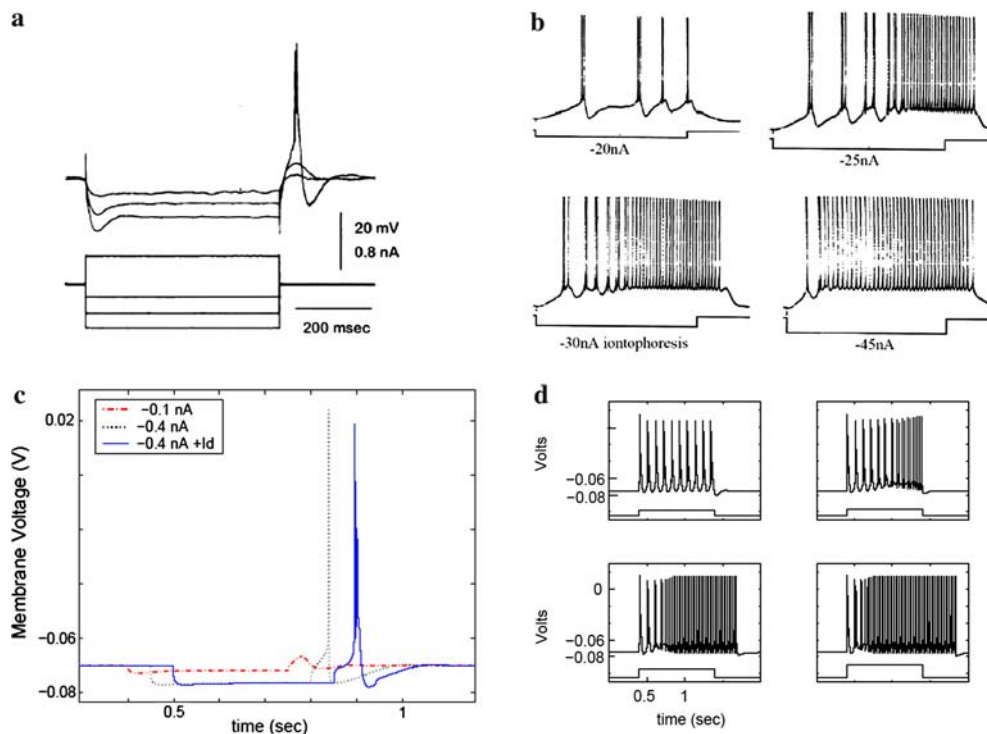


Fig. 7 Experimental and simulated firing dynamics of TL5 cells. **a** Experimental rebound response in bursting layer 5 cells (upper set of traces) after hyperpolarizing current is removed (current is shown in lower set of traces)-adapted from Castro-Alamancos and Connors (1996b) (Copyright 1996 by the Society for Neuroscience). **b** Experimental Layer 5 cell firing with increasing dendritic depolarization-adapted from Schwindt and Crill (1999) (with

permission, copyright by the American Physiological Society). **c** Simulated rebound response of a TL5 cell for increasing hyperpolarizing injected current. **d** Simulated firing response of a TL5 cell. Simulated results are based on the Wilson Type (AR-A) model. A similar behavior of the detailed Hodgkin–Huxley model (utilized in AR) is shown in Fig. S2 in Supplementary Material section

(zone A). Excitation of IN caused these cells to fire and in turn produce a long-lasting (~ 1 s) GABA_B-hyperpolarization of TL5 cell (due to the GABA_B inhibitory connection).

Stimulation Pattern 1: In the single-pair model of TL5-IN neuron (Fig. 8a), only the basal zone received excitation. This caused initially a single spike in the TL5 cell and multiple spikes in IN. The fast multiple spikes in interneuron IN effectively activated GABA_B receptors in the TL5 cell thus generating prolonged long-lasting (~ 1 s) GABA_B-based hyperpolarization in TL5. With subsequently-arriving components of the 10 Hz stimulus train, an increased rebound depolarization is observed in TL5 (due to low-threshold calcium current I_T within the cell). The TL5 cell, however, exhibited only single spikes as shown in (Fig. 8b, middle trace $I_{stim} = I_s$) with no progression to bursts, and, therefore, no AR was generated.

Stimulation Pattern 2: Here, both the apical and basal dendritic zones (A and B) received excitation. Importantly, the total drive to both zones was the same as that delivered to zone B alone in the first test, hence stimulus strength did not change from pattern 1, but

rather its delivery site is split. In this case, it can be seen (Fig. 4b, upper trace, $I_{stim} = I_s + I_d$) that the rebound response in TL5 cell is now augmented to reach multiple spikes or bursting in a manner consistent with AR experiments in (Fig. 6a, and in Castro-Alamancos and Connors 1996a). In each cycle, an arriving stimulus temporarily released the TL5 cell from inhibition. This caused increased depolarization that backpropagated to the dendritic compartment and contributed in lowering the threshold of dendritic Ca²⁺-based action potentials and, therefore, caused burst firing in the TL5 cell. Hence, AR is produced in this case.

To clarify the basic underlying mechanisms at a sub-cellular level, we investigated (1) the strength of hyperpolarization caused by slow GABA_B inhibition, (2) the role of the low threshold calcium current I_T , and (3) the effect of the stimulus frequency, on the observed AR.

As seen in Fig. 8c (upper, middle traces), by decreasing GABA_B inhibition, hyperpolarization of the cell is reduced. Therefore, the low-threshold I_T current did not de-inactivate sufficiently prior to an arriving stimulus, and only a little rebound depolarization occurred. This

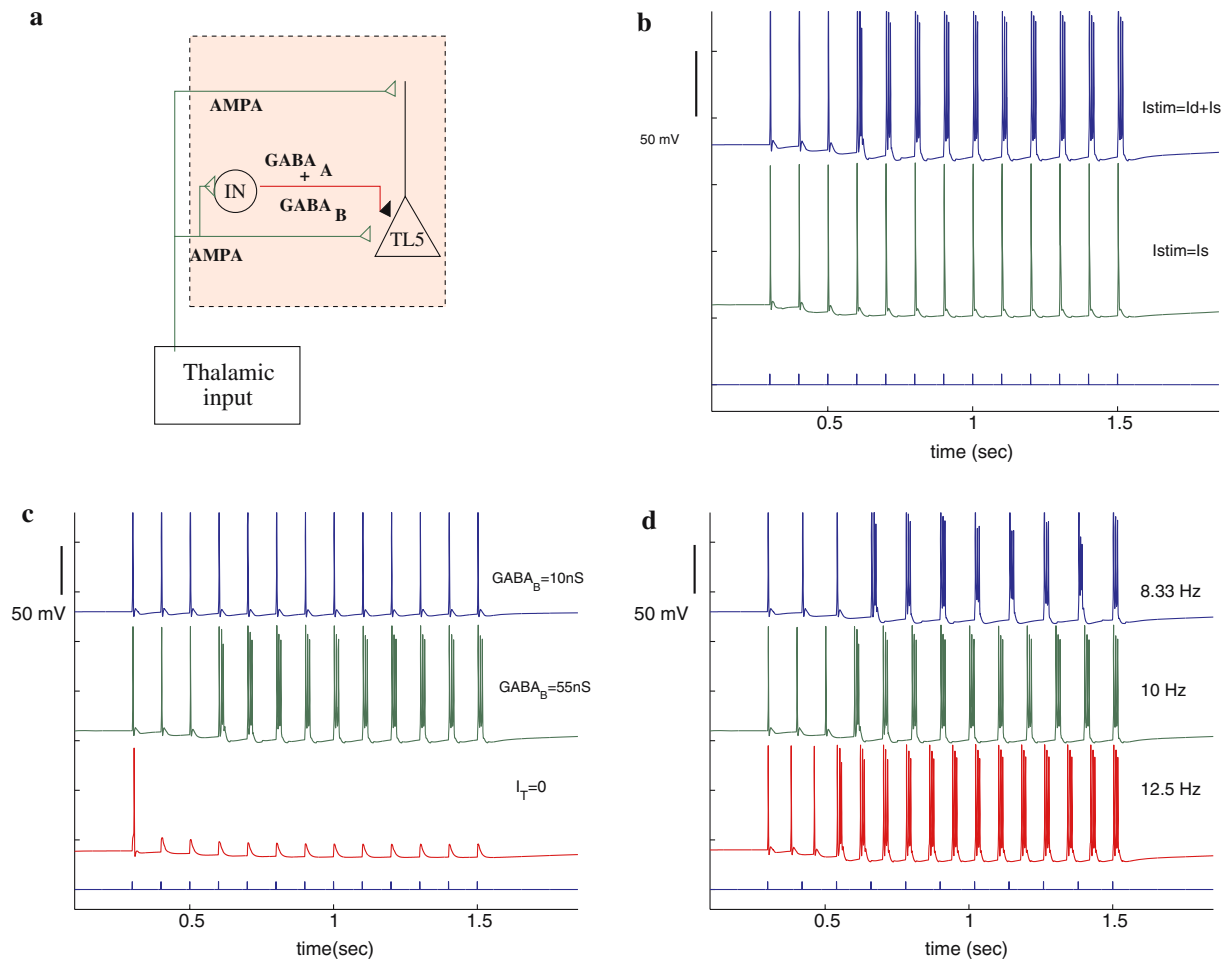


Fig. 8 Cortical augmenting responses in a single pair of TL5-IN cells in response to 10 Hz electrical stimulation (Hodgkin–Huxley dynamics AR-D). **a** Schematic of the TL5-IN pair for AR initiation. Here, thalamic input is delivered through fast excitatory (AMPA) connections. IN cells inhibit TL5 cells through fast GABA_A and slow GABA_B synapses. **b** Augmentation occurs when stimulation I_{stim} is split into both apical zone A (I_d) and

basal zone B (I_s). Middle trace I_{stim} is applied to zone B only. Lowest trace shows arrival times of the 10 Hz stimulus. **c** The cell shows weak or no augmentation when GABA_B inhibition is reduced (compare upper and middle trace). Blockage of intrinsic current I_T shows disappearance of AR (bottom trace). **d** Effect of stimulus frequency on AR

reduced rebound effectively caused a lower gain amplification, and thus no augmentation (AR) was induced.

The existence of the ionic current I_T in the cell was essential to develop AR, as seen in Fig. 8c (lower trace). By decreasing somatic I_T , the stimulus could not produce rebound depolarization in the simulated TL5 cell and, consequently, augmentation was abolished.

Finally, the AR phenomenon was sustainable for a relatively wide range of stimulus train frequencies (up to 12.5 Hz as shown in Fig. 8d), as observed experimentally. At higher frequencies, AR will only occur at alternate cycles of the stimulus train. This frequency-dependent entrainment can be understood when considering the activation dynamics of the low threshold current I_T as detailed elsewhere (Karamah 2002).

3.2.2 Multiple circuit AR demonstration

We investigated conditions under which cortico–cortical connections contribute to AR generation, as reported in animals (Steriade et al. 1991).

For computational efficiency, all cellular models used heretofore were of the Wilson-type, as explained in the supplementary material section (AR-A models).

We utilized minimal TL5 network to represent two cortical regions interconnected via long-range fibers across a hierarchical topology (Figs. 3, 9a).

Between two distant regions PL5₁ and PL5₂ (Interareal Columnar Assembly ICA), long-range cortico–cortical inputs are either feedback (green lines in Fig. 9a, b, arriving mainly in the superficial layer 1 to

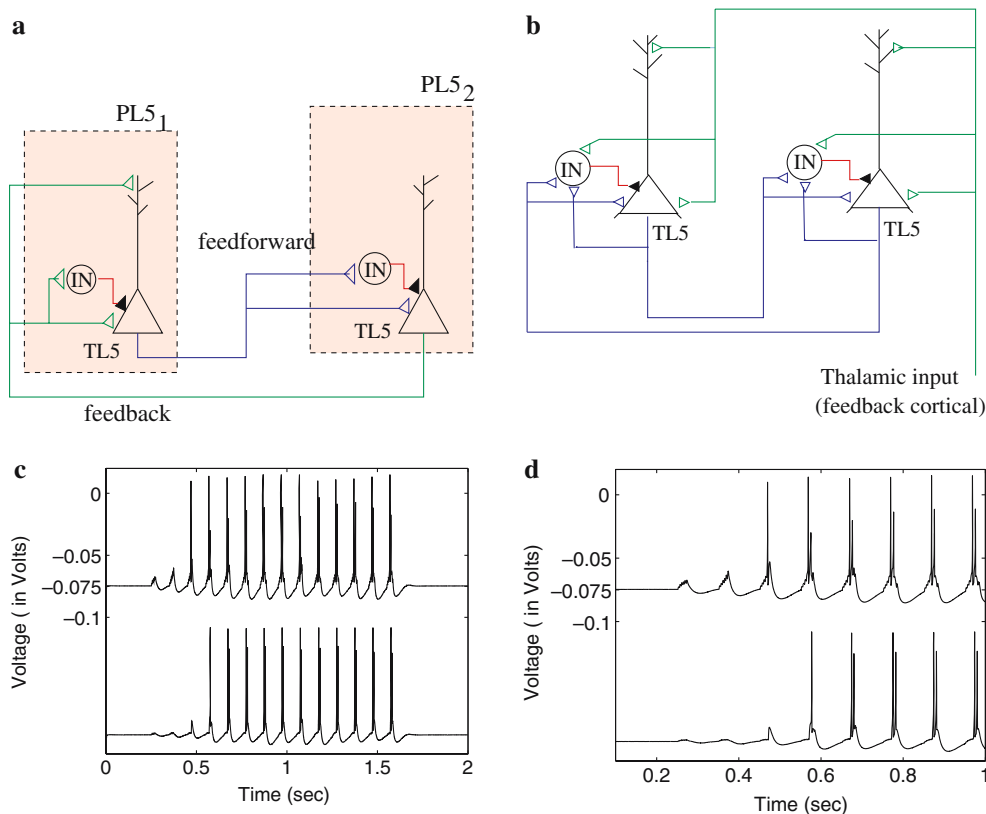


Fig. 9 Two region model of AR initiation (Wilson type dynamics AR-A). **a** and **b** show the basic two-region circuit models utilized. **a** Interconnections between two regions follow a hierarchical connection topology ($PL5_2$ is of higher order, $PL5_1$ is of lower order). **b** Connectivity within a single region. TL5-TL5 connections are

contact TL5 cells at their apical dendritic zone A), or feedforward (blue lines in Fig. 9a, arriving mainly in the middle layers to contact TL5 cells at their basal dendritic zone B as well as the adjacent interneuron IN).

Within a single region (Local Columnar Assembly LCA), TL5 cells form reciprocal excitatory connections at their basal dendritic system (Fig. 9b). TL5 cells also contact local inhibitory interneurons.

Accordingly, as seen in the first two cycles in Fig. 9c and d, a feedforward input to a model TL5 cell causes an initial fast excitation (EPSP) followed by a long-lasting $GABA_B$ mediated inhibition (IPSP) due to the firing of the associated local interneuron IN. This mimics the experimental results observed in Castro-alamancos and Connors (1996b), Steriade et al. (1998b), and Gernier et al. (1998).

Augmenting responses that occurred under ketamine anesthesia conditions in cats can also be reproduced. In particular, the stimulus train is delivered at ~ 10 Hz, only fast (AMPA) excitatory synapses were added, and the slow excitatory NMDA receptors are blocked to simulate the effect of ketamine.

AMPA mediated **c** AR will occur in cells belonging to both cortical regions. Top trace is the somatic voltage of cell from the lower order area ($PL5_1$) while bottom trace is of a cell belonging to $PL5_2$. **d** An expanded version of the plot shown in **c**

To achieve AR, we utilized TL5 neurons belonging to two hierarchically-connected cortical regions (Fig. 9a). Here, we note that the first region (consisting of $PL5_1$ neurons) is of lower order than the second region (consisting of $PL5_2$ neurons). Accordingly, connections from $PL5_1$ to $PL5_2$ arrive in zone B because they are of the feedforward type, while the reciprocal connections ($PL5_2$ to $PL5_1$) are of the descending feedback type arriving to zone A of these TL5 cells.

To understand the initiation of AR in this circuit, an external 10 Hz stimulus train (thalamic or otherwise) is assumed to arrive mainly into one cortical region ($PL5_1$). During the first few stimulus cycles, rebound depolarization in TL5 cells of that region causes an increase in activation beyond the stimulus effect and leads to single spike firing in these cells (Fig. 9c). This firing is transferred to the second cortical region $PL5_2$ in a feedforward manner causing characteristic rebound depolarization and firing in TL5 cells of that region (similar to stimulus pattern 1 in the basic circuit simulation). Firing activity from $PL5_2$ is in turn feedback onto the apical dendritic zone A of TL5 cells in $PL5_1$ which, with

subsequent input stimulus cycles, have sufficient apical dendritic excitation to fire in bursts (stimulus pattern 2 in the basic circuit simulation). This observed augmentation is qualitatively similar to what has been observed experimentally.

Note here that if the total input delivered from PL5₁ to zones A and B of PL5₂ is delivered to zone B only (with equivalent overall strength), only weak augmentation will occur with no bursting in these cells (not shown, similar to Fig. 8b).

It is therefore apparent that an intact intracortical system of connections is necessary for AR to be generated within the cortex itself. In addition, small cortical networks with little or no input to cortical layer 1 might not be able to generate cortical ARs.

3.3 Alpha-like rhythms

To simulate alpha activity, a reduced-order 6 column network model was used (intracolumnar circuit shown in Fig. 10b) with individual columns simplified to contain only layers 5, 3 and layer 5-to-layer 3 inhibition. To

simulate a more extensive layer, the boundary conditions were circular (closed chain) and each column made connections with its two nearest neighbors (Fig. 10a). Connections between columns were made by pyramidal cells of layer 3 (P3) and layer 5 (regularly spiking R5 and TL5). Cells of all layers, modeled using the Wilson type formulation, had random spontaneous synaptic activity (A-HH model, see Supplementary Material for modeling details).

3.3.1 Idling alpha

The alpha model was first simulated under low background excitation levels which were only sufficient to create occasional spikes in a simulated cell. This approximates the experimental condition of eyes closed or unfocused attention. In this case, simulations showed a dominant peak in the EEG power spectral density in the idling alpha range 8–10 Hz (Fig. 11a, solid line). This alpha behavior was faithfully reflected at the cellular level by the firing activity of various pyramidal cells (P3, TL5, and R5, Fig. 11b1). TL5 cells were, however, the pacemakers of this oscillatory behavior as they fired passively at 10 Hz mainly due to intrinsic ionic currents. This is shown next.

The critical role of TL5 cells and their intrinsic currents I_T and I_h is elucidated also in Fig. 11. First, blockade of the current I_h led to a drop in the firing frequency of TL5 cells and hence in the EEG oscillatory frequency into the delta range (~ 5 Hz) (Fig. 11a, dashed line). This can be explained by the role of this current. I_h is an inward current which brings the cell membrane voltage to depolarization levels necessary for the I_T current to activate. The removal of I_h , therefore, causes longer periods of time during which the TL5 somatic membrane voltage is in the subthreshold range for I_T activation and hence reduced cellular firing (Fig. 11b2).

Second, the blockade of both I_h and I_T currents led to the complete cessation of alpha rhythmicity (Fig. 11a, dotted line). Here, TL5 cells fired sporadically based on the low background level of excitation and the overall network activity reduced, causing no dominant spectral component.

It is important to note here that the above idling alpha rhythm is different from the AR phenomenon simulated earlier although they share a similar substrate (TL5 and IN neurons, Figs. 9a and 10b). First, unlike AR, the idling alpha *did not* involve bursting in TL5 network but was rather characterized by regular firing of single spikes in the TL5 network (Figs. 9c, 11b1). Second, the single spike firing in TL5 cells caused single spike firing in the associated local interneuron IN. In this case, the slow inhibitory GABA_B connection between IN and

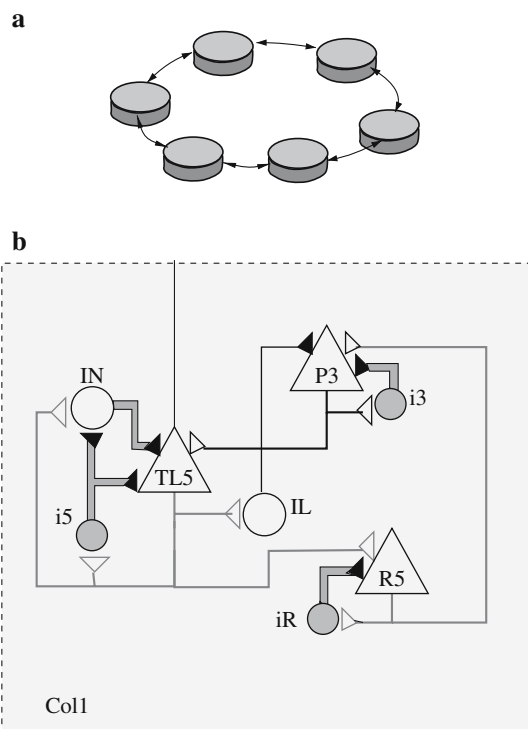


Fig. 10 **a** Six cortical columns connected in a closed chain. **b** Reduced-order circuit of a single cortical column used in the alpha, slow-wave sleep, and seizure simulations. TL5, R5, and P3 are pyramidal cells in layers 5, lower layer 5, and layer 3, respectively, with associated inhibitory interneurons (i5, iR, and i3). Parameters of various interconnections are given in the Supplementary Material section

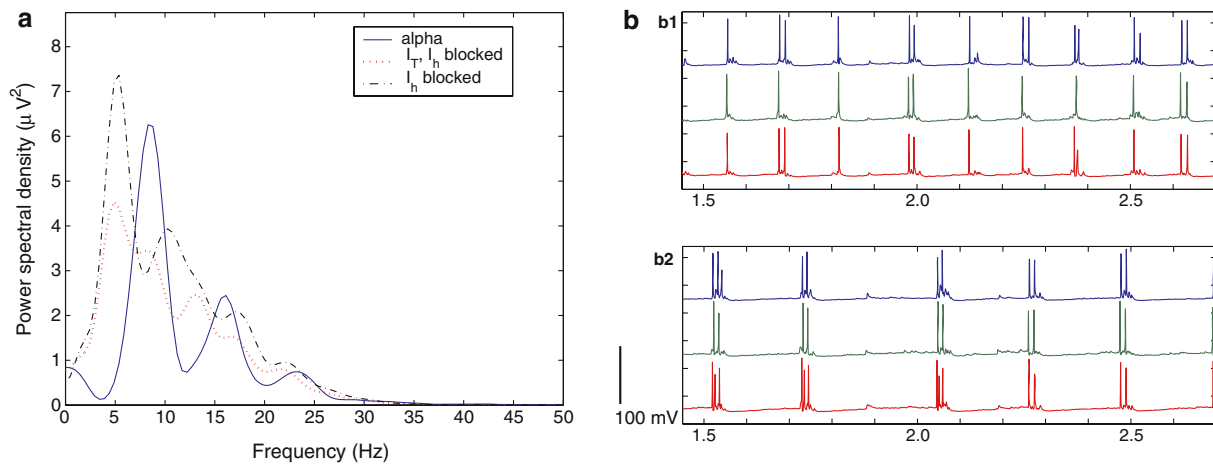


Fig. 11 Simulations of alpha oscillations in the reduced-order 6 column network of Fig. 10. **a** Power spectral density of simulated EEG rhythm. Starting from an idling alpha (8 Hz), blockade of I_T will cause a drop in main frequency. Blockade of both I_T and I_h will lead to the cessation of obvious rhythmicity. **b** Cellular firing

in the base alpha case (**b1**) and when I_h is blocked (**b2**). In both **b1** and **b2**, the top trace corresponds to Layer 3 pyramidal cell P3, the middle trace corresponds to TL5 cell, and the bottom trace to small layer 5 cells (R5) in a single column

TL5 will not be active since GABA_B receptors are maximally activated only under fast firing in IN neurons, a condition only satisfied under AR. Since GABA_B inhibition is minimal, large hyperpolarization events are absent and hence rebound depolarization in individual layer 5 cells will not occur.

Hence, unlike augmenting responses occurring at 10 Hz, the so-called idling alpha activity, while having the same neural substrate, is a passive or weak recruitment process of TL5 cells whose dynamics are distinct from the strong activation, resonance-like phenomenon observed during AR.

3.3.2 Higher frequency alpha

Functional alpha (frequency at 10–13 Hz) can be attained in the same simulation model as that of idling alpha if TL5 cells were made to burst under sufficient excitation (Fig. 12). This was demonstrated in three test cases depending on the stimulation pattern of TL5 cells. In all tests, excitation levels to other cells (P23 and R5) were kept constant.

(a) In the first test, high levels of synaptic activation arrived only onto zone B of TL5 cells. Based on the firing properties of TL5 cells, this produced regular single-spike firing in TL5 which was also transferred to other pyramidal cells (Fig. 12b1). The field potential associated with this firing behavior did not show any dominant frequency component

but rather exhibited a spectral content spread in the delta to beta frequency range (Fig. 12a, dotted line denoted as B).

(b) In the second test, the level of excitation was the same as in test 1; the inputs were however distributed into both zones A and B of TL5 cells. This allowed TL5 cells to fire in bursts (Fig. 12b2). Here, it could be seen that the field potential showed a dominant spectral peak in the upper alpha range (10–13 Hz) (Fig. 12a, solid line A+B). At the cellular level, this was reflected by a closer coherence in firing between the various pyramidal cells, paced by the bursting activity in TL5 cells.

(c) Finally, the third test involved reducing the overall excitation into zone B to 14% of the original levels with no excitation applied into zone A. As expected, this produced only single spike firing in TL5 cells (Fig. 12b2) which corresponds to idling-alpha EEG rhythm (~9 Hz) (Fig. 12a, dashed line, 0.14B). Note that this is similar to the rhythm obtained previously (compare Figs. 11b1 and 12b3). The EEG corresponding to the three different test cases (a–c) is shown in Fig. 12c which corroborates the findings at the cellular level.

In summary, the three tests show that the observed shift in the dominant alpha power between idling and functional alpha was *not* due to simple increase in background excitation level but rather due to the commencement of bursting in TL5 cells under specific stimulation patterns, mainly concurrent activation of zones A and B in these cells.

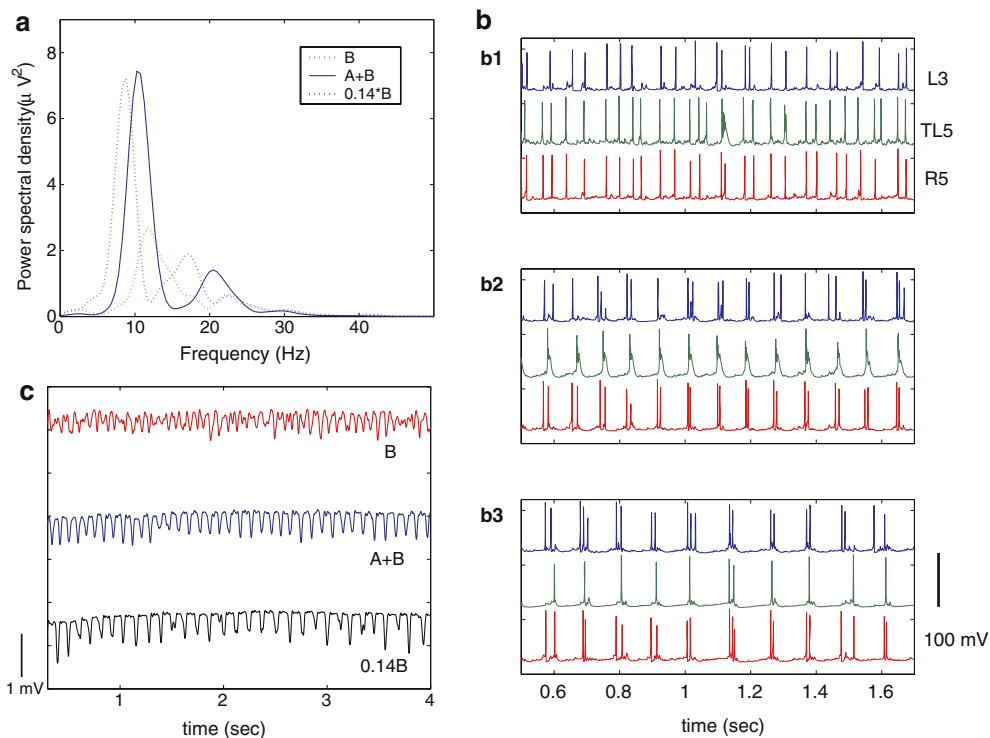


Fig. 12 Simulations of TL5 bursting effect on alpha rhythms in the reduced-order 6 column network of Fig. 10. **a** Power spectral density of simulated EEG under three TL5 excitation scenarios (see text). **b** Corresponding firing of L3, TL5 and R5 cells from a single column under three excitation scenarios. In all three cases, TL5 excitation is varied while L3 and R5 excitation is held at fixed

levels. **b1**: Excitation to zone B only causes low rhythmicity firing in a single column (*top trace* L3; *middle* TL5; *bottom* R5). **b2**: Excitation A+B causes bursting in TL5 cells (*middle trace*) which punctuates other cells in the same column. **b3**: Low excitation to zone B only produces rhythmic firing at 8–9 Hz. **c** simulated EEG for the three cases (*top* B; *middle* A+B; *bottom* 0.14B)

3.4 Slow-wave oscillations

The characteristic up and down states (depolarization and hyperpolarization, see Fig. 6b) occurring at low frequency (< 1 Hz) during later sleep stages (Sanchez-Vives and McCormick 2000) can be modeled using a reduced-order 6 column network highly similar to that used for the alpha simulations (Fig. 10a,b—columns connected in a circular chain). Here, cells of all layers had random, equal strength spontaneous synaptic activity (see Supplementary Material for details). The closed chain connectivity was used mainly to circumvent scale limitations since slow wave sleep required activation of large sets of neuronal populations. The length or size of such chain was verified, importantly, to not cause of the characteristic < 1 Hz rhythmicity observed. To approximate a larger network with reverberating activity, the strength of synaptic connections was increased from that used in the alpha model.

In the simulations, slow-wave sleep rhythms developed as cycles of neuronal silence and activation as shown in Fig. 13a for the six columns. Starting from neuronal silence, an up state was initialized by an early

firing in TL5 cells followed by wide spread cellular firing across various lamina of the cortex (Fig. 13b, asterisks). The spread of activity into layer 3 was especially dominant since the layer 5 to layer 3 inhibition (caused by LTS interneurons) was modeled to be minimal, as was observed experimentally to occur during sleep (Xiang et al. 1998).

The up state of cellular firing, which lasts for few hundred milliseconds, is subsequently terminated by a combination of factors, possibly the following.

- (a) Several intrinsic cellular ionic mechanisms, such as activation of calcium-dependent slow potassium currents $I_{K(Ca)}$, inactivation of persistent sodium currents $I_{Na,p}$ (Timofeev et al. 2000), or activation of slow adapting Na^+ dependent K current (Compte et al. 2003);
- (b) Synaptic disfacilitation, which occurs when the efficacy of neural connections decrease possibly due to the depletion of extracellular calcium. The latter is necessary for current to be injected at a synapse (Massimini and Amzica 2001).

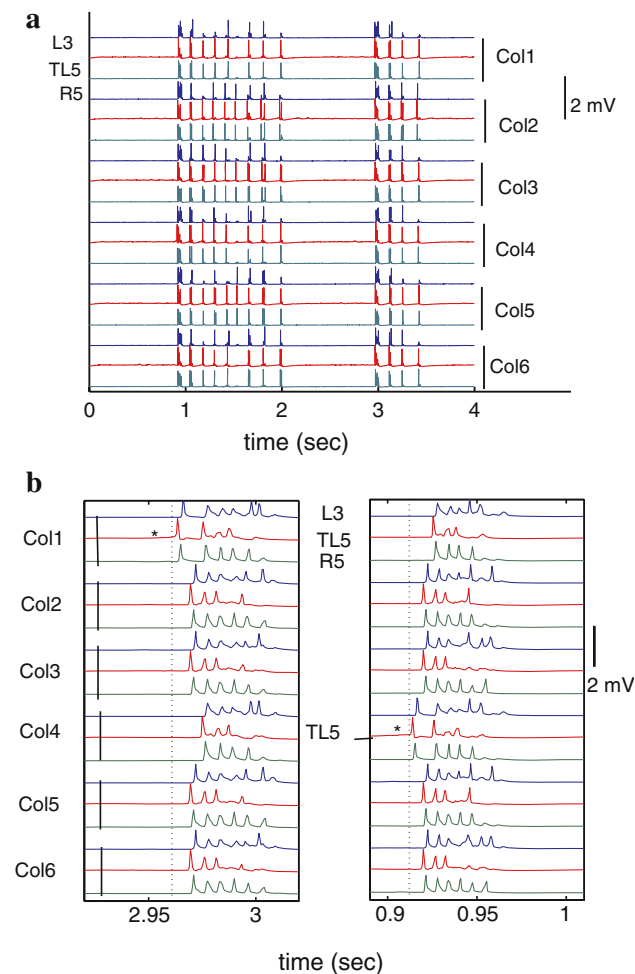


Fig. 13 Simulation of slow-wave sleep using the reduced-order 6 column network model of Fig. 10. **a** Slow wave activity is generated in the chain at around 1 Hz and is reflected across all cells after being initiated in TL5 cells. **b** An expanded view of the earlier plot shows TL5 cells precede all other neurons in firing after hyperpolarization in each cycle (*asterisk* in TL5 traces of columns 1 and 4)

In the current simulation model, the upstate was assumed to be terminated by incorporating both synaptic disfacilitation as well as an intrinsic Ca^{2+} dependent K current $I_{K(\text{Ca})}$ (adopted from Timofeev et al. 2000).

Since the termination of the upstate is well documented, our purpose here was to look closer at the “restart” mechanisms of firing or upstate initiation. It was noted through simulations that a down state was characterized by neuronal hyperpolarization (and thus neuronal silence). This hyperpolarization was terminated due to the high gain amplification property of TL5 cells. That is, when in a hyperpolarized low activity state, TL5 cells amplified their spontaneous post-synaptic currents inputs, due to the increase in inward current (I_h) under hyperpolarized conditions and low

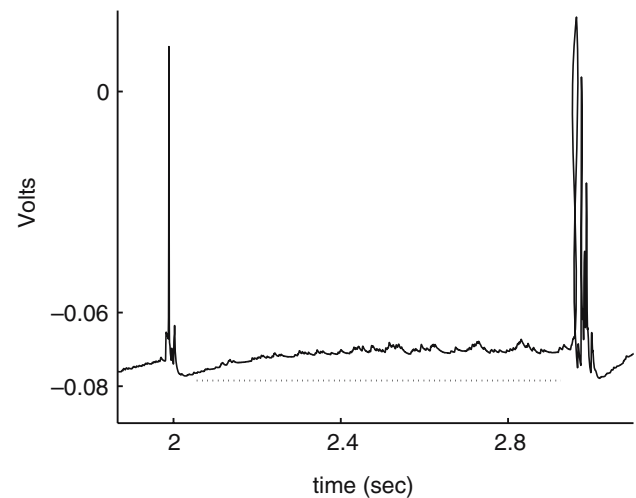


Fig. 14 An expanded view of a TL5 cell membrane potential shows increasing depolarization during the down state which culminates in oscillatory membrane potential and eventual firing. Cell was in column 1 of previous Fig. 13

threshold calcium currents (I_T) (Castro-Alamancos and Connors 1996a). Therefore, TL5 cells were the first to fire after a long period of silence. This is demonstrated in Fig. 14 by the progressive release from hyperpolarization of TL5 cells and the ensuing miniature oscillations in membrane potential just preceding cellular firing. Upon firing single spikes, TL5 cells are able to trigger discharge across the layers to which they are connected, thus initiating the up state and restarting the slow-wave cycle (Fig. 13).

3.4.1 Disinhibition-induced seizures

The characteristic spike-and-wave seizure observed experimentally when inhibition is blocked was also studied in our modeling framework. We show that the initiation of such disinhibition-induced seizure is based on the same principles of the initiation of slow-wave sleep coupled with excessive excitation or positive feedback within the network.

This was done in the reduced order 6 column model as shown in Figs. 15 and 16. In this network model, the circuit model was the same as for slow-wave (Fig. 10a,b).

Simulations showed that the early spikes of a seizure occurring after hyperpolarization (neuronal silence) are initiated in TL5 cells and are then transferred to other cortical layers. In much the same way as during slow-wave sleep, TL5 cells fired after a long period of decreasing hyperpolarization (Fig. 16a). This is in agreement with the experimental observations of the current source density profiles and cellular membrane voltage recordings during seizures in Castro-Alamancos (2000).

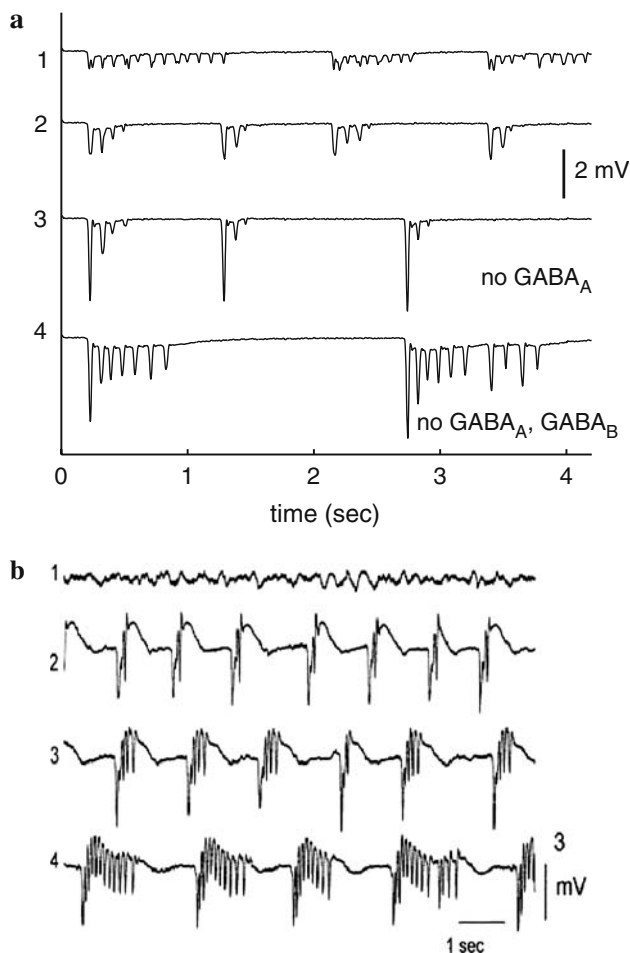


Fig. 15 Simulation of disinhibition-induced seizures using the same reduced order 6 column network model of Fig. 10. **a** spike component of the experimental rhythm is qualitatively replicated in the model upon removal of fast $GABA_A$ (traces 2,3) then slow $GABA_B$ inhibition (trace 4). **b** Disinhibition-induced seizure experimentally observed in the cortex under increasing disinhibition (traces 2 and 3 show increased $GABA_A$ blocking, trace 4 show $GABA_B$ blocking, from (Castro-Alamancos, 2000, Copyright 2000 by the Society for Neuroscience)

Starting from a slow-wave sleep condition (trace 1 in Fig. 15a), an increasing blockade of fast inhibitory $GABA_A$ receptors decreased somatic inhibition in TL5 which, due to unconstrained excitation levels, could then produce very strong burst-like firing (or what is known as paroxysmal depolarizing shifts, PDS) at around 10–12 Hz frequency (traces 2,3 in Fig. 15a).

Burst-like firing in TL5 cells produced similar high levels of fast firing in associated interneurons IN, which in turn lead to strong activation of slow acting $GABA_B$ mediated inhibition in the network. This occurs since, (1) IN interneurons are connected back to TL5 cells by slow $GABA_B$ inhibitory receptors, and (2) $GABA_B$ receptors are maximally activated when subjected to

high frequency firing in IN interneurons, a condition which does occur in this seizure case.

Therefore, with burst-like PDS firing in TL5 cells, intact $GABA_B$ inhibition was maximally activated, thus creating very large hyperpolarizing potentials in TL5 and subsequently terminating PDS oscillations. The occurrence of large hyperpolarization is plausible since experimental evidence found a $GABA_B$ receptor protein to be highest in cortical layers 5 and 6b (rat somatosensory cortex, Princivalle et al. 2000) indicating a large concentration of such receptors in these layers.

In the final test, $GABA_B$ inhibition was also blocked. In this case (trace 4 in Fig. 15a), the TL5 cells continued to produce burst-like PDS firing since no hyperpolarizing currents are available. Therefore, the membrane potential, and the corresponding field potential, continued to produce fast runs at ~ 10 –12 Hz until disfacilitation in the cellular connections occurred due to mechanisms similar to those controlling slow-wave sleep (see above). The prolonged unchecked oscillations effectively increased the period of the disinhibition induced-seizure, as observed experimentally (Fig. 15b).

The role of slow $GABA_B$ inhibition in this seizure type was further elucidated by varying the conductance strength of $GABA_B$ receptors (Fig. 16b). While fast $GABA_A$ inhibition is blocked as before, we reduced the maximal conductance $g_{GABA_B, \max}$ to 50% of its original value. This resulted in longer periods of fast runs (Fig. 16b, trace 2) compared to the runs associated with unaltered $g_{GABA_B, \max}$ conductance (Fig. 16b, trace 1), indicating an significant role of $GABA_B$ receptors in controlling the TL5 network excitation and reducing the length of a seizure cycle.

4 Discussion

We have presented a framework of models whereby the intrinsic dynamics of the cerebral cortex itself are taken into account. At a fine scale, these models replicate the firing dynamics of single TL5 cells and thereby of neocortical columns as observed in experimental recordings. They then show the relevance of such dynamics, when a TL5 network is properly connected as a local and interareal columnar assembly (LCA and ICA), to the genesis of several EEG rhythms.

The demonstration that a simplified architecture of neocortical circuitry can account for a number of low frequency phenomena supports the suggestion of accumulating experimental evidence that such rhythms owe a significant portion of their genesis to the cortex rather than principally to the thalamus or other deeper brain systems. Still, the latter structures clearly exert power-

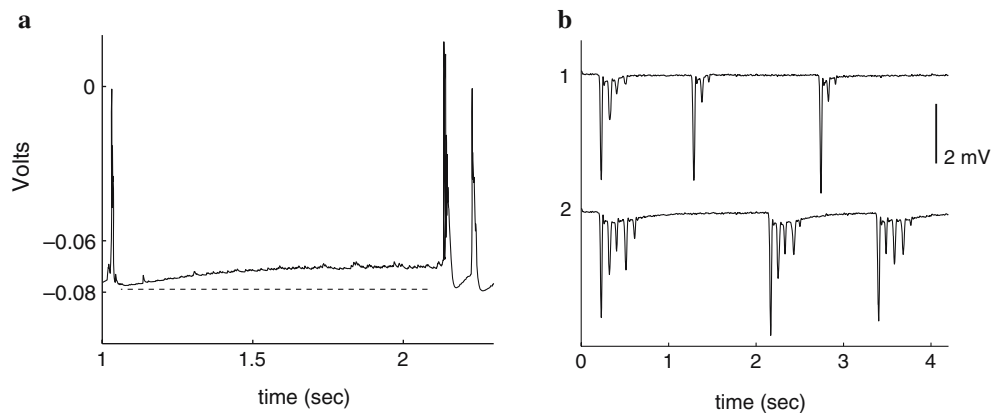


Fig. 16 **a** Membrane potential of a TL5 cell during interseizure lulls is characterized by increasing depolarization leading to PDS-like firing. **b** Decreasing GABA_B inhibition allows for longer period of oscillations. *Top trace* $g_{\text{GABA}_B, \text{max}} = 330 \text{ nS}$, *bottom trace* $g_{\text{GABA}_B, \text{max}} = 110 \text{ nS}$

ful influences on EEG as well. The presented framework facilitates investigation of the nature of the local cortical, distant cortical and subcortical interactions in EEG production.

Augmentation

The model explains augmenting responses occurring in cortical tissue as a consequence of coupling intrinsic TL5 cellular mechanisms with specific input activation patterns. In particular, the model predicts that inputs to some cortical areas can cause resonance-like activation, or fast initiation and spread of excitation, when three main conditions occur (1) such inputs target TL5 cells at their basal zone B as well as the associated local IN interneurons, in effect hyperpolarizing the TL5 cell and thereby enabling high gain amplification (rebound depolarization), (2) the inputs also target TL5 cells at their apical zone A, allowing such cells to produce bursts when recovering from hyperpolarization, (3) the inputs are delivered at a repetition rate of 10–12 Hz thus exploiting an intrinsic rate of resonance within TL5 cells due to interaction of intrinsic ionic currents (I_T and I_h).

The necessity of two interacting input streams in AR generation and the critical role of TL5 cells in this interaction is consistent with various experiments reporting cortical AR both at the thalamus-to-cortical and cortico-cortical levels.

- (a) In thalamo-cortical induced AR, stimulation of the thalamic VL nucleus, but not VPL thalamus, induced cortical AR which was accompanied by rebound depolarization and bursting in layer 5 cells (sensorimotor cortex of rats, Castro-Alamancos

and Connors 1996a,b). In light of modeling here, this distinct behavior ties with the different projection patterns of both nuclei. In fact, VL thalamus avoids layer 4 and projects to layers 1 and 5 (zones A and B) while VPL projects to middle layers (zone C).

- (b) In cortico-cortical induced AR, patterns of collaterally projecting layer 5 cells also avoided middle layers and stimulation of such fibers induced bursting type, sustained augmentation (Nunez et al. 1993).
- (c) In a series of experiments and modeling studies, augmenting responses could not be generated in small cortical slices, and hence AR was attributed to be thalamic in origin (Bazhenov et al. 1998a,b; Gernier et al. 1998). In view of our model, this could be explained by an inadequate targeting of zones A and B in the TL5 network. In particular, it is plausible that a small neocortical slice will not possess intact connections to zone A the TL5 cells, which was a critical factor in the modeled AR generation. That is, the interareal columnar assembly ICA scale, or inputs mimicking its projection pattern, seems to be essential for AR generation.

Alpha rhythms

The model explains idling alpha rhythms as due to single spike firing in TL5 cells caused by intrinsic currents in these cells (I_T and I_h), and thus confirms earlier simulations of this rhythm (Jones et al. 2000). It is further predicted here that idling rhythms shift to the delta range ($\sim 5 \text{ Hz}$) when the I_h current is blocked within the cell.

More importantly, the model preliminarily accounts for the previously-unexplained so-called functional

alpha rhythms occurring in the upper alpha range (10–12 Hz) that are reported in cognition experiments (Mima et al. 2001; Basar et al. 2001). In particular, the model predicts that such functional alpha rhythms could originate in a TL5 network when it undergoes burst firing, and as such reflect a different phenomenon than the common idling alpha which is expressed by single spike firing in this network. The ability of large TL5 cells to burst in vivo at frequencies up to 12 Hz was observed experimentally (Steriade et al. 2001). We propose that “functional” alpha could possibly be a reflection of selective recruitment, mediated by bursting, at the local columnar assembly LCA scale (as discussed in detail elsewhere in subsequent publication).

Slow-wave sleep and Seizures

Both the slow-wave sleep and disinhibition-induced seizures are EEG oscillations characterized within a single cycle by a period of prolonged neuronal firing followed by a period of neuronal silence. For both rhythms, the framework predicts that TL5 cells play an integral role in restarting the oscillation cycle following neuronal silence.

During the latter periods of neural inactivity, expressed as “down” state of the cycle at the EEG level, TL5 cells undergo periods of increased hyperpolarization which cause such cells to become high-gain amplifiers of any subsequent spontaneous activity. This amplification property allows TL5 cells to be slowly released from hyperpolarization and leads to subsequent TL5 cell firing. By virtue of its network connections, TL5 firing then spreads over wide neuronal populations both vertically within a column (layer 5 to layer 3) as well as horizontally within the local columnar assembly LCA.

Experimentally, slow-wave oscillations were recently demonstrated in situ with activation initiated in layer 5 and propagated to layers 6 and 2,3 in absence of thalamic input (Sanchez-Vives and McCormick 2000). The vertical spread of activity could also be enhanced by the reduction of layer 5 to layer 3 inhibition during sleep as reported (Xiang et al. 1998).

During periods of neuronal firing, expressed as “up” state of the cycle at the EEG level, slow wave sleep is characterized by a progression of several rhythms (spindles followed by gamma activity, which is not modeled here). While spindles (10–14 Hz) are mainly generated in the thalamus (Contreras et al. 1997), a TL5 network could follow such rhythms at least in the lower frequency range. Further more, experiments show that, at later stages of sleep, delta waves (3–4 Hz) of EEG were faith-

fully traced by bursting of TL5 cells (Nunez et al. 1993, not modeled here).

When cortical inhibition is progressively blocked, an “up” cycle of the slow-wave sleep is transformed into a seizure-like state where fast runs (10–14 Hz) of paroxysmal depolarizing shifts (PDS) can be seen. The model predicts such runs to be expressed at the TL5 cell level as very strong bursts (PDS-like) in these cells, whose duration is controlled by the level of slow GABA_B inhibition available.

This is in agreement with experiments where disinhibition-induced seizures in rats progressed from slow-wave sleep and showed paroxysmal discharge patterns (PDS) initiated within layer five (Castro-Alamanos 2000) the period of which was dependent on hyperpolarization levels.

Note here that it is also possible that a network of smaller layer 5 cells (not simulated here) with doublet firing behavior (Schubert et al. 2001) could sustain even faster oscillations (12–14 Hz) such as spindles occurring in slow-wave sleep (Contreras et al. 1997) as well as the 10–15 Hz runs reported in some seizures (Steriade et al. 1998) when the excitatory drive is left unchecked.

Comparison to other modeling approaches

This investigation attempts to develop a single coherent framework within which all EEG rhythms may be eventually understood. It is unique in sketching a basic cortical architecture which could account for the generation of several low frequency rhythms.

The intermediate level of modeling detail used here is also unique as it enables a somewhat broader and more integrated *systems-level* view than has been available previously. This hybrid framework could potentially allow bridging between three main approaches in brain rhythm analysis: *abstract generalized* models of EEG generation, *detailed neurocomputational* models of single neural rhythms, and *theoretic* models of cortical information processing.

First, abstract generalized models explore single EEG phenomena with limited or no emphasis on cortical structure. Examples of these include alpha genesis in thalamocortical neurons (Lopes da Silva 1991) where alpha activity is produced by generic approximate dynamics neuronal populations, and the global EEG model where brain electric potential signals are propagating waves over a continuum of neuronal matter (Nunez 1995) and other field theoretic EEG models (Katzenelson 1982; Wright et al. 1995).

Second, detailed neurocomputational models generally explore single phenomena and are based on fairly accurate models of individual neurons. As such, these

simulation models are quite tailored and have no clear extensions to reproducing other rhythms. For example, some models represent the cortex as a homogeneous structure of interacting neurons (slow-wave sleep models in Timofeev et al. 2000 and Compte et al. 2003). Others consider network phenomena that produce idling alpha activity only (Jones et al. 2000). Still others focus mainly on the thalamus as the underlying oscillator with the cortex echoing the thalamic oscillations (thalamic AR in Bazhenov et al. 1998a,b; spindles in Contreras et al. 1997).

Finally, theoretic models of cortical information processing explore average neuronal activity to explain specific cognitive tasks (Raizada and Grossberg 2003). These models generally do not emphasize the real-time individual neuronal firing dynamics or their heterogeneity.

The current framework links the three levels of modeling. First, it looks at EEG as the electric field potential signature of neural processing. This is supported by the correspondence between neuronal firing and EEG oscillation profiles under many vigilance states in awake animals (Destexhe et al. 1999a; Steriade et al. 2001). Second, it incorporates detailed intrinsic cellular dynamics of the cortex which explain EEG rhythms at the cell firing level (similar to cortical alpha model in Jones et al. 2000). Third, it looks at cortical network phenomena necessary to sustain such rhythms (similar to thalamic networks in Contreras et al. 1997). It finally incorporates non-homogeneous cortical connections at three spatial scales with direct functional meaning (columnar, local columnar assemblies, and interareal columnar assemblies). It therefore lends itself to theoretical studies of cortical information processing. The functional role of the developed neurocircuit and scales as these relate to some forms of cognitive processing will be addressed elsewhere in subsequent publications (functional alpha).

Limitations

Because the framework retains a significant amount of detail in its representation of fundamental and identifiable cortical neurocircuit anatomy and physiology, it is amenable to considerable experimental testing in its current form. However, certain limitations are worth noting.

(a) *Thalamic role:* Thalamic nuclei were not included explicitly in our model; however, their oscillatory role has been studied intensively. We believe, based on our assessment of the dynamic behavior of tha-

lamic oscillator models (Bazhenov et al. 1998a,b; Contreras et al. 1997) that these could be integrated into our circuit model to yield a more complete thalamocortical system. This would likely be able to account for an even wider range of EEG observable phenomena, such as the interaction between thalamic spindles and cortical TL5 network during different vigilance states, the role of thalamic circuitry in initiating alpha rhythms, and others.

(b) *Modeling framework:* In the presented simulations, the model used for each rhythm was a subset of the same larger framework where TL5 cell dynamics are the skeleton of the neurocircuit. We therefore have considerable confidence that these sub-models behaviors are in fact representative of different operational modes of a single large cortical model. However, this must be verified using a full scale detailed neuro computational model, which is not the main purpose of this research exercise. In fact, to produce a full scale model requires addressing the following:

1. *Data availability:* certain detailed physiological data are often not available (e.g. for TL5 cells), are difficult to obtain (in vivo recordings), or are simply too computationally expensive to incorporate. However, we found that the current framework model was sufficient to account for the qualitative EEG features detailed above. The results should be able to serve as a guide for designing efficient large-scale models.
2. *The issue of scale:* Testing with various numbers of cortical columns and various individual cell models (Hodgkin–Huxley and Wilson types) suggested strongly that the primary effect of using a relatively limited number of neurons (up to 54) was that the strength of synapses needed to be set at suprphysiological levels to represent large numbers of synapses. This issue is the same as that encountered by a number of single EEG phenomenon models (e.g. Jones et al. 2000). A primary effect here is that the EEG generated was susceptible to artifacts produced by individual units, though these did not appear to alter the basic dynamics of the neurocircuit. In any case, employing more populous and ionic-current-accurate models of the same structure should allow more accurate weighting of synaptic strengths, greater subtlety in EEG feature production, and less vulnerability to spurious cell-dependent noise.

We had currently undertaken an effort to model several of the above phenomena in greater detail (e.g. AR) with larger number of neurons. This effort is increasingly advocating the utility of the presented integrative approach of modeling which spans the three levels of studying the brain electric activity, abstract generalized models, detailed neurophysiological, and information-processing based.

Acknowledgements We thank R. McCarley for reviewing the manuscript. This work was funded by NSF under the KDI grant IBN-9873478 and by DARPA under the MICA grant 6893375, and by the AUB URB grant 588321. E. Brown was supported by NIH grants MH59733, MH61637, NIH grant R01 DA015644, and NSF grant IBN-0081548.

References

- Armstrong-James M, Fox K, Das-Gupta A (1992) Flow of excitation within rat barrel cortex on striking a single vibrissa. *J Neurophysiol* 68:1345–1358
- Basar E, Basar-Eroglu C, Karakas S, Schurmann M (2001) Gamma, alpha, delta, and theta oscillations govern cognitive processes. *Int J Psychophysiol* 39:241–248
- Bazhenov M, Timofeev I, Steriade M, Sejnowski TJ (1998a) Computational models of thalamocortical augmenting responses. *J Neurosci* 18:6444–6465
- Bazhenov M, Timofeev I, Steriade M, Sejnowski TJ (1998b) Cellular and network models for intrathalamic augmenting responses during 10 Hz stimulation. *J Neurophysiol* 79:2739–2748
- Burger T, Larkum ME, Luscher H-R (2001) High I_h channel density in the distal apical dendrite of layer V pyramidal cells increases bidirectional attenuation of EPSPs. *J Neurophysiol* 85:855–868
- Burger T, Senn W, Luscher, H (2003) Hyperpolarization-activated current I_h disconnects somatic and dendritic spike initiation zones in layer V pyramidal neurons. *J Neurophysiol* 90(4):2428–2437
- Brumberg J, Pinto D, Simons D (1999) Cortical columnar processing in the rat whisker-to-barrel system. *J Neurophysiol* 82:1808–1817
- Bush P (1995) Compartmental models of single neurons and small networks in the primary visual cortex of the cat. PhD dissertation, University of California, San Diego
- Callaway EM (1998) Local circuits in primary visual cortex of the macaque monkey. *Annu Rev Neurosci* 21:47–74
- Castros-alamancos MA, Connors B (1996a) Cellular mechanisms of the augmenting response: short-term plasticity in a thalamocortical pathway. *J Neurosci* 16:7742–7756
- Castro-Alamancos MA, Connors B (1996b) Spatiotemporal properties of short term plasticity in sensorimotor thalamocortical pathways of the rat. *J Neurosci* 16:2767–2779
- Castro-Alamancos MA (2000) Origin of synchronized oscillations induced by neocortical disinhibition in vivo. *J Neurosci* 20:9195–9206
- Caulier LJ, Clancy B, Connors BW (1998) Backward cortical projections to primary somatosensory cortex in rats extend long horizontal axons in layer I. *J Comp Neurol* 390:297–310
- Chen W, Zhang JJ, Hu GY, Wu CP (1996) Electrophysiological and morphological properties of pyramidal and nonpyramidal neurons in the cat motor cortex in vitro. *Neuroscience* 73:39–55
- Contreras D, Destexhe A, Sejnowski TJ, Steriade M (1997) Spatiotemporal patterns of spindle oscillations in cortex and thalamus. *J Neurosci* 17:1179–1196
- Compte A, Sanchez-Vives MV, McCormick DA, Wang X-J (2003) Cellular and Network Mechanisms of slow oscillatory activity (<1 Hz) and wave propagations in a cortical network model. *J Neurophysiol* 89:2707–2725
- Destexhe A, Bal T, McCormick DA, Sejnowski TJ (1996) Mechanisms underlying synchronized oscillations and propagating waves in a model of ferret thalamic slices. *J Neurophysiol* 76:2049–2070
- Destexhe A, Mainen Z, Sejnowski TJ (1998) in Koch C, Segev I (ed) *Methods in neuronal modeling*, pp 1–25. MIT, Cambridge
- Destexhe A, Contreras D, Steriade M (1999) Spatiotemporal analysis of local field potentials and unit discharges in cat cerebral cortex during natural wake and sleep states. *J Neurosci* 19:4595–4608
- Destexhe A (2001) LTS cells in cerebral cortex and their role in generating spike-and-wave oscillations. *Neurocomputing* 38:555–563
- Durstewitz D, Seamans JK, Sejnowski TJ (2000) Dopamine-mediated stabilization of delay-period activity in a network model of prefrontal cortex. *J Neurophysiol* 83:1733–1750
- Feldmeyer D, Sakmann B (2000) Synaptic efficacy and reliability of excitatory connections between the principal neurons of the input (layer 4) and output layer (layer 5) of the neocortex. *J Physiol* 525:31–39
- Fellman DJ, Van Essen DC (1991) Distributed hierarchical processing in the primate cerebral cortex. *Cereb Cortex* 1:1–47
- Galarreta M, Hestrin S (2000) Burst firing induces a rebound of synaptic strength at unitary neocortical synapses. *J Neurophysiol* 83:621–624
- Gernier F, Timofeev I, Steriade M (1998) Leading role of thalamic over cortical neurons during postinhibitory rebound excitation. *Proc Natl Acad Sci USA* 95:13929–13934
- Ghazanfar A, Nicolelis M (1999) Spatiotemporal properties of layer V neurons of the rat primary somatosensory cortex. *Cereb Cortex* 9:348–361
- Goldberg JH, Lacefield CO, Yuste R (2004) Global dendritic spikes in mouse layer 5 low threshold spiking interneurons: implications for control of pyramidal cell bursting. *J Physiol* 558.2:465–478
- Hefti B, Smith P (2000) Anatomy, physiology, and synaptic responses of rat layer V auditory cortical cells and effects of intracellular GABA-a blockade. *J Neurophysiol* 83:2626–2638
- Helmchen F, Imoto K, Sakmann B (1996) Ca^{2+} buffering and action 1173, 1992. potential-evoked Ca^{2+} signaling in dendrites of pyramidal neurons. *Biophys J* (70):1069–1081
- Huguenard JR, McCormick DA (1992) Simulation of the currents involved in rhythmic oscillations in thalamic relay neurons. *J Neurophysiol* 68:1373–1383
- Jones SR, Pinto DJ, Kaper TJ, Kopell N (2000) Alpha-frequency rhythms desynchronize over long cortical distances: a modeling study. *J Comput Neurosci* 9:271–291
- Kaneko T, Cho R, Li Y, Nomura S, Mizunp N (2000) Predominant information transfer from layer III pyramidal neurons to corticospinal neurons. *J Comp Neurol* 423:52–65
- Karamah F. N. (2002) A model for cerebral cortical neuronal group electric activity and its implications for cerebral function. PhD dissertation (MIT, 2002), Cambridge
- Katzenelson RD (1982) Deterministic and stochastic field theoretic models in the neurophysics of EEG. PhD dissertation, UCSD

- Kawaguchi Y, Kubota Y (1997) GABAergic cell subtypes and their synaptic connections in rat frontal cortex. *Cereb Cortex* 7:476–486
- Klimesch W (1999) EEG alpha and theta oscillations reflect cognitive and memory performance: a review and analysis. *Brain Res Rev* 29:169–195
- Larkum ME, Zhu JJ, Sakmann B (1999a) A new cellular mechanism for coupling inputs arriving at different cortical layer. *Nature (Lond)* 398:338–341
- Larkum ME, Kaiser KMM, Sakmann B (1999b) Calcium electrogenesis in distal apical dendrites of layer 5 pyramidal cells at a critical frequency of back-propagating action potentials. *Proc Natl Acad Sci USA* 96:14600–14604
- Larkum ME, Senn W, Lüscher H-R (2004) Top-down dendritic input increases the gain of layer 5 pyramidal neurons. *Cereb Cortex*. DOI: 10.1093/cercor/bhh065
- Lopes da Silva F (1991) Neural mechanisms underlying brain waves: from neural mechanisms to networks. *Electroencephalogr Clin Neurophysiol* 79:81–93
- Markram H (1997) A network of tufted layer 5 pyramidal neurons. *Cereb Cortex* 7:523–533
- Massimini M, Amzica F (2001) Extracellular calcium fluctuations and intracellular potentials in the cortex during the slow sleep oscillation. *J Neurophysiol* 85:1346–1350
- McCormick D, Huguenard J (1992) A model of the electrophysiological properties of thalamocortical relay neurons. *J Neurophysiol* 68:1384–1400
- Mima T, Oluwatimlehin T, Hiroaka T, Hallet M (2001) Transient interhemispheric neuronal synchrony correlates with object recognition. *J Neurosci* 21:3942–3948
- Mormann F, Elger CE, Lehnertz K (2006) Seizure anticipation: from algorithms to clinical practice. *Curr Opin Neurol* 19(2):187–193
- Mouncastle VB (1998) *Perceptual neuroscience, the cerebral cortex*. Harvard University press, Cambridge
- Nunez A, Amzica F, Steriade M (1993) Electrophysiology of cat association cortical cells in vivo: intrinsic properties and synaptic responses. *J Neurophysiol* 70:418–429
- Nunez P (1981) *Electric fields of the brain*. Oxford University Press, Oxford
- Nunez P (1995) *Neocortical dynamics and human EEG rhythms*. Oxford University Press, Oxford
- Princivalle AP, Pangalos MN, Bowery NG, Spreafico R (2000) Distribution of GABA(B) receptor protein in somatosensory cortex and thalamus of adult rats and during postnatal development. *Brain Res Bull* 52:397–405
- Raizada RD, Grossberg S (2003) Towards a theory of the laminar architecture of cerebral cortex: computational clues from the visual system. *Cereb Cortex* 13(1):100–113
- Rhodes P, Gray CM (1994) Simulations of intrinsically bursting neocortical pyramidal neurons. *Neural Comput* 6:1086–1110
- Rhodes P, Llinas R (2001) Apical tuft input efficacy in layer 5 pyramidal cells from rat visual cortex. *J Physiol* 536:167–187
- Sanchez-Vives M, McCormick D (2000) Cellular and network mechanisms of rhythmic recurrent activity in neocortex. *Nat Neurosci* 3:1027–1034
- Schubert D, Staiger JF, Cho N, Kotter R, Zilles K, Luhmann HJ (2001) Layer-specific intracolumnar and transcolumnar functional connectivity of layer V pyramidal cells in rat barrel cortex. *J Neurosci* 21:3580–3592
- Schwandt P, Crill W (1999) Mechanisms underlying burst and regular spiking evoked by dendritic depolarization in layer 5 cortical pyramidal neurons. *J Neurophysiol* 81:1341–1354
- Sinton CM, McCarley RW (2000) Neuroanatomical and neurophysiological aspects of sleep: basic science and clinical relevance. *Semin Clin Neuropsychiatry* 5(1):6–19
- Spain W, Schwandt P, Crill W (1991) Post-inhibitory excitation and inhibition in layer V pyramidal neurons from cat sensorimotor cortex. *J Physiol* 434:609–626
- Steriade M, Amzica F, Neckelmann D, Timofeev I (1998) Spike-wave complexes and fast components of cortically generated seizures. II. Extra- and intracellular patterns. *J Neurophysiol* 80:1456–1479
- Steriade M, Timofeev I, Gernier F, Durmuller N (1998b) Role of thalamic and cortical neurons in augmenting responses and self sustained activity: dual intracellular recordings in vivo. *J Neurosci* 18:6425–6443
- Steriade M, Timofeev I, Gernier F (2001) Natural waking and sleep states: a view from inside neocortical neurons. *J Neurophysiol* 85:1969–1985
- Tallon-Baudry C, Bertrand O (1999) Oscillatory gamma activity in humans and its role in object representation. *Trends Cogn Sci* 3(4):151–162
- Tamas G, Buhl E, Lorinz A, Somogyi P (2000) Proximally targeted GABAergic synapses and gap junctions synchronize cortical interneurons. *Nat Neurosci* 3:366–371
- Thomson A, Deuchars J (1997) Synaptic interactions in neocortical local circuits: dual intracellular recordings in vitro. *Cereb Cortex* 7:510–522
- Thomson A, Bannister A (1998) Postsynaptic pyramidal target selection by descending layer III pyramidal axons. *Neuroscience* 84:669–683
- Timofeev I, Grenier F, Bazhenov M, Sejnowski TJ, Steriade M (2000) Origin of slow cortical oscillations in deafferented cortical slabs. *Cereb Cortex* 10:1185–1199
- Tung A (2005) New anesthesia techniques. *Thorac Surg Clin* 15(1):27–38
- Van Brederode J, Spain W (1995) Differences in inhibitory synaptic input between layer II–III and layer V neurons of the cat neocortex. *J Neurophysiol* 74:1149–1166
- Wang Z, McCormick D (1993) Control of firing mode of corticocortical and corticopontine layer V burst-generating neurons by Norepinephrine, acetylcholine and 1S,3R-ACPD. *J Neurosci* 13:2199–2216
- Wang X-J (1999) Fast burst firing and short-term synaptic plasticity: a model of neocortical chattering neurons. *Neuroscience* 89(2):347–362
- Williams S, Stuart G (1999) Mechanisms and consequences of action potential burst firing in rat neocortical pyramidal neurons. *J Physiol* 521:467–482
- Wilson H (1999) Simplified dynamics of human and mammalian neocortical neurons. *J Theor Biol* 200:375–388
- Wright JJ, Lilet DT (1995) Simulation of electrocortical waves. *Biol Cybern* 72:347–356
- Wu J-Y, Guan L, Yuang T (1999) Propagating activation during oscillations and evoked responses in neocortical slices. *J Neurosci* 19:5005–5015
- Xiang Z, Huhuenard J, Prince D (1998) Cholinergic switching within neocortical inhibitory networks. *Science* 281:985–988